In presenting the dissertation as a partial fulfillment of the requirements for an advanced degree from the Georgia Institute of Technology, I agree that the Library of the Institute shall make it available for inspection and circulation in accordance with its regulations governing materials of this type. I agree that permission to copy from, or to publish from, this dissertation may be granted by the professor under whose direction it was written, or, in his absence, by the Dean of the Graduate Division when such copying or publication is solely for scholarly purposes and does not involve potential financial gain. It is understood that any copying from, or publication of, this dissertation which involves potential financial gain will not be allowed without written permission.

7/25/68

DESIGN AND PRELIMINARY TESTING OF A PREMIXED FLAT-FLAME BURNER INCORPORATING AN OPPOSED GAS PARTICLE JET

A THESIS

Presented to

The Faculty of the Graduate Division

by

Mohammad Amin Shakill

In Partial Fulfillment

of the Requirements for the Degree

Master of Science in Mechanical Engineering

Georgia Institute of Technology

April, 1970

DESIGN AND PRELIMINARY TESTING OF A PREMIXED FLAT-FLAME BURNER INCORPORATING AN OPPOSED GAS PARTICLE JET

Approved:

Chairman

Date approved by Chairman: 20 April 1970

ACKNOWLEDGMENTS

I would like to express my appreciation to those who contributed their help and encouragement to this work. I particularly wish to express my gratitude to my major professor, Dr. Pandeli Durbetaki, the faculty advisor for this thesis, whose guidance, inspiration, understanding and encouragement, not only in the pursuit of this thesis but in all aspects of my graduate career, have led to the completion of this work.

I wish to acknowledge with appreciation the constructive comments and time given by my thesis reading committee members, Dr. Prateen Desai and Dr. Warren C. Strahle.

The help given by Mr. Joseph G. Doyal and Mr. Bobby L. Wallace, the laboratory and machine shop technicians, is especially appreciated.

In particular, I am grateful for the friendship of my office mates, Mac D. Bowen and Alex Alkidas, and the opportunity to share their ideas in this work.

Finally, I would like to express my sincere appreciation to my wife, Charlene, for her continued support and understanding.

TABLE OF CONTENTS

LIST OF TABLES

LIST OF ILLUSTRATIONS

* Photographic Figures

LIST OF ILLUSTRATIONS Continued

---

* Photographic Figures

LIST OF ILLUSTRATIONS Continued

SUMMARY

This work deals with the use of a flat-flame burner which incorporates an opposed flow particle injector for the study of ignition and burning of metal particles.

Dilute streams of aluminum powder, consisting of particles with an average size of 50 micrometers in diameter were introduced into the laminar flow of hot gases. A flat-flame burner with an opposed flow particle injector was designed for the generation of hot gases and the injection of metal particles in this hot gaseous medium. The objective was to carry out preliminary tests with the designed experimental apparatus and to find out if ignition of metal particles would be possible by such an instrument.

Methane and air were used as the reactant gases, to burn in a flat-flame, and to produce the desired hot medium for the ignition and burning of metal particles. Aluminum particles were diluted with an inert gas, nitrogen, acting as a carrier; and the stream of nitrogen with the aluminum particles suspended in it was introduced into the hot oxidizing medium at atmospheric pressure.

The ignition of aluminum particles with the apparatus used was observed and photographed. The results of some preliminary measurements are discussed. Pictures and photographs are presented as documentary evidence of the ignition of the aluminum particles in this designed experimental system. Temperature measurements of the hot gases in the presence or absence of aluminum particles were made.

It was observed that the aluminum particles were ignited when the average temperature of the flame was as low as 1500°F.

CHAPTER I

INTRODUCTION

Statement of the Problem

Studies in the use of metals as a fuel and the associated investigations relating to the ignition and burning characteristics of metals have received great momentum during the last two decades. Da Rosa (1)* was probably the first who proposed metals as a rocket fuel. Research in this field has been intensified under the stimulus of new technological developments. The advantage of using metals as fuel for technological applications rests entirely on their very large heat of combustion, the attainment of high temperature and production of intensive transient or continuous light emission. The use of metals in propulsion has stimulated research on ignition and burning processes, particularly of metal powders.

Workers in this field of combustion have accomplished a great deal on the subject of ignition and burning of certain metals such as magnesium, aluminum, and beryllium which have been recognized as rocket propellant additives because of their smaller molecular weights. In spite of the accomplishments in this field, complications have always existed because information about the reaction mechanism; the formal laws of kinetics; and the laws of macroscopic phenomena, including the mechanical motion of burning metals, are still limited

---

*The numbers in parentheses correspond to the numbers in the Bibliography.

and further investigations in the field are definitely needed.

The general purpose of the research activities initiated with this work (in our laboratories) is to develop a system and appropriate experimental techniques to study the ignition and burning of particles with the prime emphasis on combustion of metal particles, initially. The objective of the present work was to design and evaluate such a system consisting of a premixed flat-flame burner utilizing an opposed flow particle injection jet.

Methane was chosen as the fuel to premix with the oxidizer (air) in a mixing chamber; the mixed gases discharged through a porous bronze plate and form the flat-flame at the top of this plate. Nitrogen was chosen as the carrier gas to introduce the particles from the opposite direction into the flame. Aluminum powder was used which provided solid sphere particles with an average size of 50 micrometers.

The experience gathered from this activity is expected to serve as a guide in planning the work to follow as well as modifications on the experimental set-up and techniques.

Background

Some aspects of metal combustion and a review of the research which has been carried out in this area have been reported by Markstein (2). Combustion of aluminum particles has been the subject of fairly extensive recent investigations and has been reviewed by three workers in the field during the last four years (2,3,4). The results of most recent investigations in this area are summarized below.

A considerable amount of work has been carried out on the

experimental determination of ignition temperatures of metals and particularly that of aluminum. The mechanism of autoignition of metals in an oxidizing atmosphere is divided into four categories by Bhan (5). Accordingly, the most fundamental mechanism of autoignition is the spontaneous accelerating oxidation of a pure metal surface in a potentially oxidizing atmosphere, i.e., pyrophoricity. Very small particle sizes are required for this process to lead to autoignition. Another mechanism is the spontaneous reaction of the oxidizing atmosphere with some very reactive intermediate chemical compounds formed from the surface of the metal which also leads to autoignition. Metals with high chemically reactive bonds are required for this mechanism. Also induced mechanical energy (e.g., friction or rupture energy) might make the metal react with an oxidizing atmosphere and lead to autoignition of the metal. Finally, electrostatic charging of particles which are isolated from the ground may occur due to friction (Tribo-electric effect) (5,6). The accumulated charges may be sufficient to cause a local electric field near the break-down value of the gas, and the resulting spark may be sufficient to raise the particle temperature to its autoignition point.

The ignition characteristics of metals depends on the formation of the protective oxide. Metals such as magnesium, which do not form the protective oxide and which generally follow zero or first order reaction and low temperature reaction rates, usually ignite below the metal melting point. On the other hand, those metals which form a protective oxide, such as aluminum and beryllium, ignite above the

metal melting point (7,8).

Kuehl (7,9) investigated the ignition and burning of metals at elevated temperatures and studied the behavior of the oxide coating which is formed during oxidation of the metals. The ignition and combustion of aluminum and beryllium wires were tested, and it was concluded that the ignition temperature is directly proportional to the square of the particle diameter. This conclusion was also noted by Friedman and Macek (10,11) as a result of their theoretical and experimental investigations. Kuehl found qualitatively that in the low pressure range (between 5 to 10 psia) ignition of aluminum particles always takes place in the vapor phase.

It should be noted at this point that Markstein (2,12) proposed that metals generally burn by heterogeneous reaction which is an important consequence of the presence of condensed-phase reactants and products. Thus, unless the metal is vaporized artificially, ignition is always preceded by reaction at the surface or on and within a protective oxide layer.

Kuehl also found that the explosive mode of combustion of aluminum wires occurs at high pressures and oxygen concentration, thus confirming the dependence of the ignition and burning of aluminum on the pressure. He defines a critical pressure as the pressure below which the metal vapor pressure becomes more important than the metal oxide melting point. A knowledge of the critical pressure as well as the surface effects of the oxidizer species are important in the determination of the ignition temperatures.

The vapor-phase combustion model was proposed and used by

Brzustowski and Glassman (8,13,14,15) and attempts were made for the experimental justification of this model by many other researchers in the field (4,7,9,11).

The high speed photographic investigations made by Drew, Prentice, and Christensen (16) on the combustion of aluminum particles in flames show that the combustion zone of aluminum particles in a carbon-monoxide flame is twice as large as that in a H_2 - O_2 flame. The authors have provided a more detailed photographic examination of the complete burning process of aluminum particles in which the motion phenomena such as jetting, spinning, and fragmentation were observed.

The photographic observations of Friedman, Macek, and Semple (17) on the combustion of aluminum and beryllium, support the events observed by Drew, et al. (16). The former observed the bubbling and fragmentation of the particles in the later stages of combustion in a H_2 - O_2 atmosphere.

Drew, Gordon, and Knipe (18) found that the existence of water vapor and consequently hydrogen in a combustion process of aluminum is largely responsible for any surface oxidation that may occur during ignition.

Macek (4) studied the ignition and burning of aluminum and beryllium particles which were injected into a gaseous environment of known composition and temperature. He found that the process which leads to the ignition of both metals is strongly affected by the physical properties of the stable oxides. The results of these investigations indicate that both metals burn by the vapor-phase mechanism. Macek investigated also the ignition and burning of

aluminum particles both in hydrogen free (dry) atmosphere as well as an atmosphere containing hydrogen (moist). He observed that aluminum particles in the presence of hydrogen burn on the surface of a liquid bubble of alumina. The observed combustion characteristics of aluminum particles such as jetting, spinning, bubble formation, and fragmentation (which are also known as burning characteristics of the group of metals which form protective oxide layer) lead to the concept of a previously proposed surface burning model (19,20).

The observation made by different investigators (4,10,11,16,17, 21,22,23,24) on the ignition and burning of aluminum (and other metals showing the same burning characteristics) leads to the conclusion that the combustion zone and the parent particle are not spherically symmetric. The spinning of a particle is due to the inhomogeneities (which are not axially symmetric) on the surface of the metal particle. This inhomogeneity is either due to the partial removal of the metal oxide from the surface by the bubble blowing process, or by the deposition of oxide on the surface as condensation during the period of self-sustained combustion. This experimental evidence indicates that the proposed vapor-phase combustion model (spherically symmetric combustion model) discussed earlier cannot be strictly followed, and the phenomena of jetting, spinning, etc. also shows that this model is not favorable. Nevertheless, it is still believed (4,7,24,25,26, 27) that the vapor-phase model is more applicable than the surface burning model, even though the latter explains jetting, bubble formation and blowing, shedding of oxide spheres, agglomeration of oxide at one side of the particle, spin, and fragmentation phenomena.

Among other things, experimental apparatus and techniques are critical in the research activity concerned with the combustion of metal particles. In the ignition and burning of aluminum and beryllium particles, most investigators (4,10,11,18) have taken the advantage of a laminar, one dimensional flow of hot gases of known and uniform characteristics and generated by a premixed flat-flame on a circular porous metal burner. Friedman and Macek (10,11) were probably the first to use the above technique in the ignition and burning of a single aluminum particle. It was found that aluminum particles will ignite when the temperature of the gas stream reaches $2300^{o}k$.

The ignition model for aluminum particles, proposed by Friedman and Macek (10,11) is based on the dominant mode of laminar heat transfer by conduction between the hot gaseous environment and the particle before ignition. The model was proved to be satisfactory by other investigators (4,7,9,13,17).

Another experimental apparatus used for the ignition and burning of metals is the flash heating system developed by Nelson, et al. (28). Using the same system, Prentice (29,30) studied the spinning, jetting, and fragmentation of aluminum particles burned by pulses of radiation from an Nd-glass laser in air and O_2 - Ar mixtures. It was found that the droplet spins, jets, radiates less intensely, and falls more rapidly in air than in the O_2 - Ar mixtures. Since the only difference between the two oxidizing atmospheres was the substitution of Argon for nitrogen in the gas mixtures, nitrogen may be participating as a reacting species; furthermore, the accumulation of a condensed

phase product during combustion in air (but not in O_2 - Ar) might be responsible for the above phenomena. Existence of hydrogen in air (moist air) can also be a factor in the above observations (4,31). Therefore, in the combustion of aluminum particles in air at atmospheric pressure, both the physical and chemical evaluation of oxide on the surface of the droplet may be necessary; and the chemical composition of the products should be studied more closely. On this basis, Prentice suggests that the studies made by other investigators (4,32,33,34) should be re-examined from the chemical point of view for the possible complications due to transient or end products other than simply metal-oxide compounds.

Even though attention has been focused on the ignition and burning of aluminum, beryllium, and magnesium, researchers have investigated the burning characteristics of other metals such as zirconium, lithium, calcium, sodium, titaniu, etc. Nelson (35,36, 37,38) used the flash heating technique mentioned above for the burning of metals which employs the use of simple intense pulses of light from a capacitor discharge-lamp to form and burn droplets of metals over a wide range of temperature and experimental conditions. He suggested that the combustion of metals such as Zr, Ta, Ti, MO, W, Pu, Sm, Re, and Al can be investigated by this method. Nelson worked with zirconium in air and mixtures of O_2 - Ar using this technique. When burning in O_2 - N_2 (air) mixtures, he found that although the final product may be the metal oxide only, both gases participate in the combustion process. It appears then that the explosion and fragmentation of metals, when burning, are due to the

presence of nitrogen (nitrogen is not necessarily the only gas which can cause fragmentation (39)) and other gases which form impurities. The phenomena such as spear point and super-cooling which occur beyond the normal explosion time (which is of the order of 10-20 msec for 50μ particle (28)) can be studied by having a smooth combustion process. This process can be attained by carefully removing the nitrogen or other gases which cause the impurities.

Experimental studies conducted with zirconium have shown that a high temperature luminous fog layer in the shape of a spherical zone is formed in which liquid oxide particles nucleate and grow from a mixture of zirconium bearing vapors emitted from the droplet and surrounding oxygen molecules (40). From the above observation it can be concluded that zirconium may burn in a vapor-phase. The vapor-phase combustion model can be extended to the study of the combustion of zirconium.

Nelson's flash-heating technique permits investigations on the burning of metals but not on the ignition phenomena. Also, the ambient gas pressure was restricted to one atmosphere and the particles were burned in cold ambient gas which contrasts with the rocket environment.

Beal, et al., (41) studied the explosive characteristics of molten metals. Zirconium was burned in air and phenomena such as jetting, fragmentation, and oxide smoke were observed. No explicit model defining the combustion characteristics of zirconium has been proposed at this time (35,36,37,38,40,41).

Rhien (42) conducted a series of combustion experiments using

lithium, beryllium, magnesium, calcium, boron, aluminum, cerium, mischmetall, titanium, zirconium, thorium, and manganese powders in nitrogen-carbondioxide. His aim was to investigate the aspects of potential suitability of these materials as fuels for propulsion in the atmospheres of Mars and Venus. Except for boron, it was found that all of the above mentioned metals ignite in carbon-dioxide and each in a different range of temperatures. From the above metals, aluminum, magnesium, chromium, and manganese did not burn in nitrogen. The most promising metal fuels that might be used in atmospheres consisting of N_2 - CO_2 mixtures are found to be very fine powders of lithium and beryllium while at the same time aluminum and magnesium also have potential.

Morison and Scheller (43) investigated the spectral characteristics of hydrocarbon-air flames containing aluminum, magnesium, and boron. In the case of aluminum, it was found that in addition to considerable continuum radiation from Al and Al_2O_3, molecular radiation from the AlO green system is also present. Therefore, visible emission from flames containing aluminum may be primarily attributed to continuum radiation from hot metal or metal oxide particles. However, the strong hand of AlO produces substantial emission in visible and/or the ultraviolet.

Seleznev, et al., (44) developed an optical method for the measurement of the burning surface temperature of condensed systems. They observed that the addition of aluminum particles to a condensed substance such as ammonium per-chlorate results in a rise of temperature, flame temperature, the amount of heat emitted in the direction

of the combustion surface, and the radiation flow from the surface.

Marshall, et al., (45) studied experimentally the drag coefficient of burning aluminum droplets. They observed that the aluminum particles burning in air, puff, spiral, and then fragment. Also the motion of the droplet relative to the stagnant gas created a crescent shaped flame zone. A rapid expansion of the vapor-phase diffusion flame is associated with the primary puff after which the flame disappears.

Remarks

Investigations in the field of metal combustion are still in the forefront. Different opinions exist concerning whether such metals as aluminum and beryllium which form a protective oxide layer burn on the surface in which case the oxidation rate is limited by the slow diffusion of reacting ions (metal and oxygen ions), or they burn in a vapor phase in which case the rate is controlled by the diffusion of the oxydizer through the gas.

Although most investigators favored the vapor-phase combustion model for the burning of aluminum and beryllium, this model cannot explain several of the phenomena that have been observed. On the other hand, occurrences such as bubble formation, vigorous fragmentation, appearance of sharp particle tracks, and geometrical assymetry lend more suitably to the concept of surface burning.

There are many factors such as purity of the metal, gas composition, the oxydizing species and concentration, inert gas species, ambient temperature, heating source and rate, total pressure, past history of the metal, the experimental apparatus

and technique, velocity past the surface, and geometry which enter the problem of ignition and the nature of metal combustion. The need for more extensive research in this field is very much apparent.

CHAPTER II

EXPERIMENTAL EQUIPMENT AND TECHNIQUES

In chapter one the metal particle combustion activity was summarized and the need to explain some of the complications and produce a better understanding of the phenomena that have been observed was clearly demonstrated.

In reviewing the literature, the need for a more effective fuel that would provide more heat, higher temperatures, and more intensive light for propulsion devices became evident. At the same time, the use of metal particles as an additive to other combustible material has been shown to be satisfactory and to meet most of these needs. Consequently, research activities to develop experimental techniques and methods for particle combustion have been initiated in our laboratories.

The main objective of this phase of the research activity was the design of a preliminary equipment set-up to be subsequently evaluated, modified and used for studies in the ignition and burning of metal particles. The apparatus which will be discussed in detail in this and other chapters to follow culminated as a result of this initial effort. The system incorporated the flat-flame burner, which provides the needed hot gaseous reactive region, and a nozzle, which introduces the metal particles into this region.

The Burner

Except for the particle injector, the flat-flame burner used in our laboratory is similar in construction to those used previously for different research purposes (10,11,17,18,46,47,48,49,50,51,52,53, 54,55,56,57). Figure 1 shows the main experimental lay-out of the system including the flat-flame burner assembly. Figure 2 shows a close-up of the burner and the incorporated particle injection system.

A schematic diagram of the burner is shown in Figure 3. A steel pipe (c), 10 inches i.d. and two feet long was used as a calming section as well as a mixing chamber. It carries six layers of 200 mesh stainless steel screens (d). The screens were mounted at a distance of 1.5 inches apart from each other. Two small holes (b), 1/8 inches in diameter were drilled near the bottom of the mixing chamber for the fuel and air passages.

The nozzle (e) was cast from aluminum and mounted at the mouth of the mixing chamber to serve as a transition section. The brass tube burner (h) is 3.28 inches i.d. and 14.5 inches long and was threaded to the transition nozzle. A 30 mesh stainless steel screen (i) was fixed inside of the burner tube at a distance of approximately 3.5 inches from the bottom of the burner tube. Solid spherical glass beads, 3 mm in diameter were added to the top of the stainless steel screen, (j). These beads fill up about 7.5 inches of the tube, leaving 3.5 inches of free space for the air-fuel mixture before it exits into the reaction region at the top of the flat-flame burner.

A Sintered porous bronze circular plate (k) was attached to

Figure 1. Experimental Set-Up of the System and the Burner Assembly.

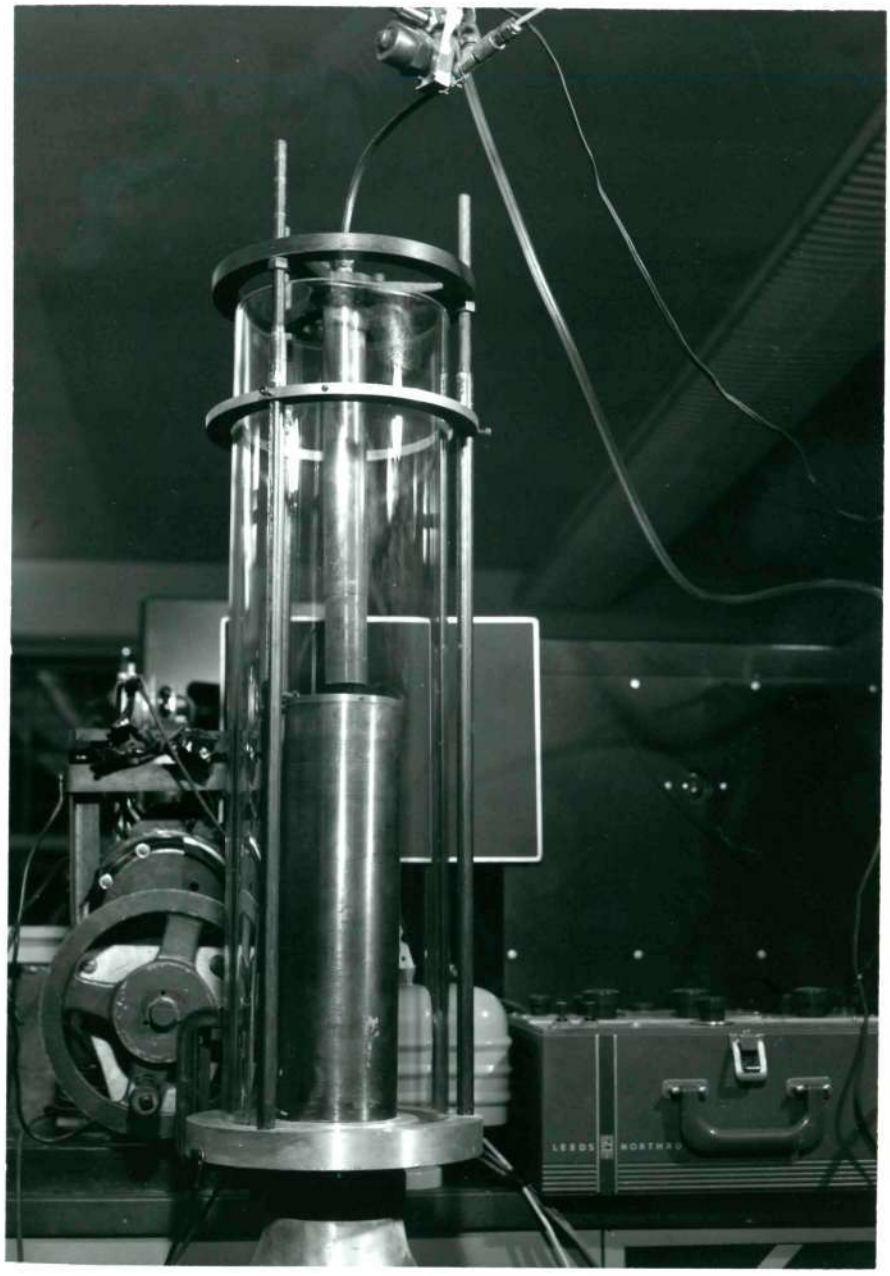

Figure 2. A Close-Up View of the Burner Tube and the Injection Nozzle.

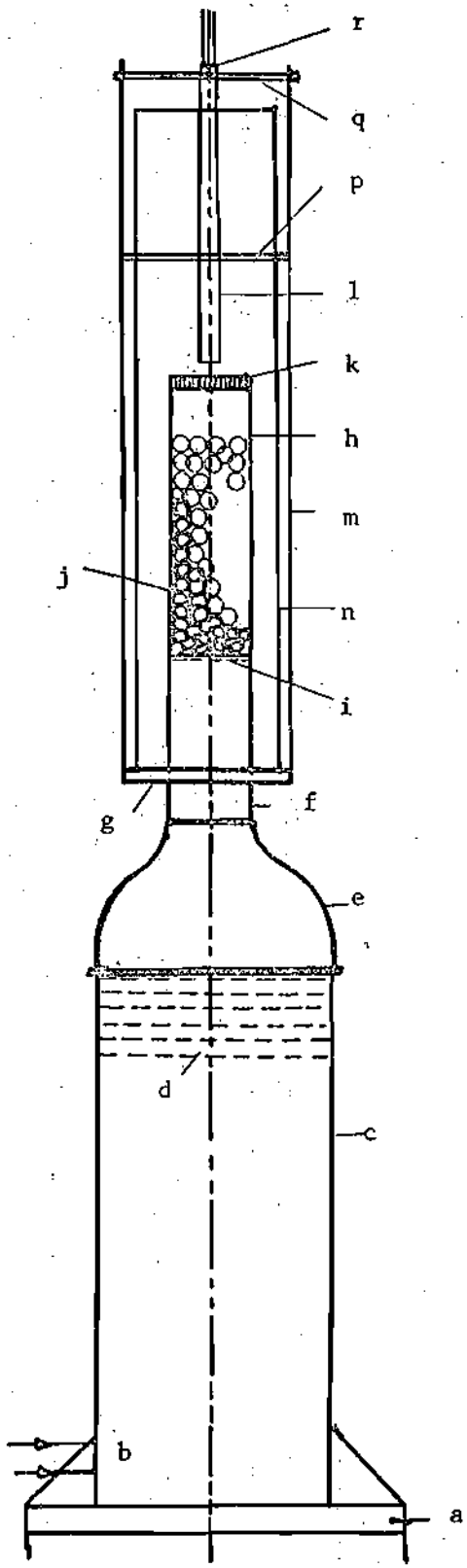

a. Carriage
b. Gas Passages
c. Mixing Chamber
d. 200 Mesh Stainless Steel Screen
e. Transition Nozzle
f. Steel Cylindrical Ring
g. Supporting Table
h. Burner Tube
i. 30 Mesh Stainless Steel Screen
j. Solid Spherical Glass Beads
k. Sintered Porous Bronze Plate
l. Particle Injection Tube
m. Supporting Rods
n. Pyrex Glass Chimney
p. Supporting Ring for the Chimney
q. Supporting Disk for the Particle Injection Tube
r. Particle-Entrance Nozzle (see Figure 4)

Figure 3. Schematic Diagram of the Flat-Flame Burner and the Incorporated Opposed Gas Particle Injection Nozzle.

the upstream end of the brass burner tube with a holder ring. This ring was fitted inside the burner tube and secured properly with screws to prevent any gas leakage around it.

A pyrex glass tube (n), 5.9 inches i.d. and 23 inches long, enclosing the burner tube, the injection nozzle, and the combustion area, as well as serving as a chimney, was incorporated in the system (see Figure 2). The pyrex glass tube is supported by a disk (g) at the bottom and a ring (p) at the top. The supporting disk (g), made of aluminum, is fitted on a steel cylindrical ring (f) at the neck of the transition nozzle, where the burner tube is fixed to the nozzle. The disk has openings for cool atmospheric air passage. It also carries three ½ inches by 30 inches steel rods (m) to form with the upper ring (p) the complete supporting structure of the pyrex glass chimney.

A stainless steel tube (l), 12 inches long and one inch i.e., was built to serve as a nozzle and introduce the metal particles into the flame. The particle injection tube was attached to a steel table (support q) and mounted axially with the burner tube on the three rods (m). The injection tube and its supporting table can be adjusted axially by six nuts.

The injection tube incorporated in our experimental apparatus is the main modification brought about, which distinguishes this flat-flame burner system from other equipment built and used in studies of the ignition and combustion of metal particles.

The oxidizer (air) and the fuel (methane) enter into the mixing chamber (c) through the holes (b) and after passing through

the screens (d), they are directed to the burner tube (h) by the transition nozzle (e). The screens in the mixing chamber and the glass beads in the burner tube serve to mix the gases and remove any velocity distribution in the flow inside the burner. The random flow of the reactants, after they leave the glass bead region, is streamlined and a uniform flow was obtained by the porous bronze plate (k) at the mouth of the burner. The gas mixtures, when ignited, form the flat-flame above the porous bronze disk and remain out of contact with any part of the burner. The pyrex glass chimney serves to keep the flame from severe outside disturbances. Air at room temperature surrounds the system and was the only coolant for it.

Nitrogen was used to dilute the aluminum powder and act as a carrier to the particles. A feed line was connected to the injection tube to introduce this mixture through the entrance nozzle (r). This nozzle was built of steel with an opening in the shape of a frustum of a cone on the inside (see Figure 4), fitted firmly into the particle injection tube and secured by screws from the top.

An oversized rectangular steel plate was welded on the bottom of the mixing chamber. The entire burner assembly is mounted through this plate to the carriage (a). The carriage was made of steel angle irons and it was provided with casters and vertically mounted bolts. Any vertical adjustment as well as leveling of the burner assembly can be made through use of the bolts.

Auxiliary Instrumentation

The experimental equipment described in the previous section represents the main part of the apparatus. Supporting instrumentation

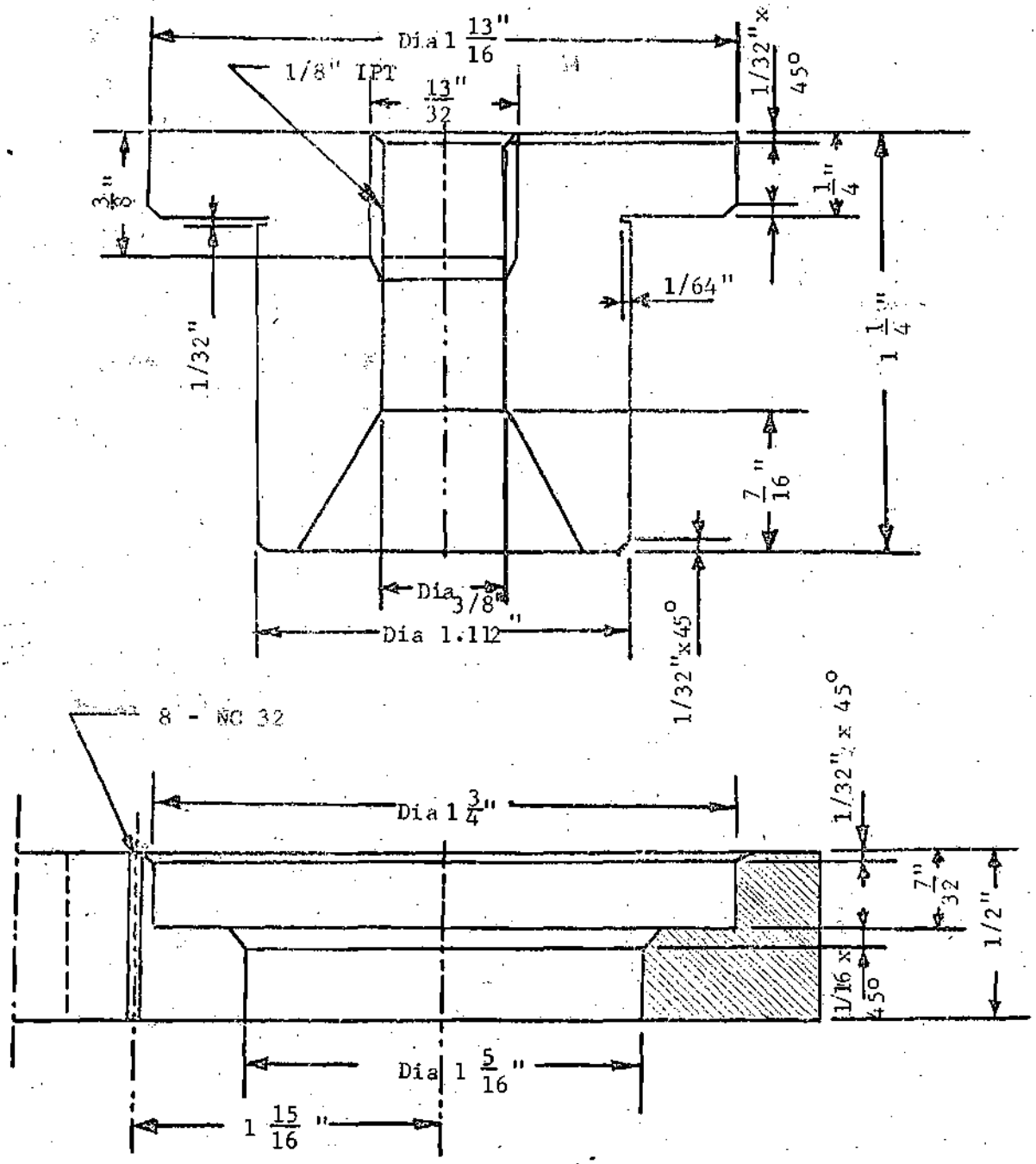

Figure 4. Detail Drawing of the Injection Nozzle Entrance Configuration and the Supporting Ring.

will be discussed in this section. The schematic diagram presented in Figure 5 shows the total experimental lay-out.

It was discussed earlier that pre-mixed methane and air were used to produce the flat-flame on the upstream side of the porous bronze plate. The fuel, methane (Matheson, grade cp 99 per cent min.), was supplied in high pressure steel containers (1). A two stage pressure regulator (2) was mounted on the fuel cylinder for pressure reduction and preliminary control of the flow. A variable area flowmeter (3) was connected downstream of the pressure regulator to measure methane flow rate. The flowmeter was also furnished with a needle valve on the upstream side of the meter. This valve was used for the precise adjustment of the flow. A 24 inch water manometer (4) and a mercury thermometer (5) mounted on the downstream side of the flowmeter provided the necessary pressure and temperature measurements respectively for the correction of the fuel flow readings.

The air for the combustible mixture of the burner was furnished from a 80 - 125 psia main line. From this line the air was directed through a filter (6) for particle removal and reduction of moisture. A single stage pressure regulator (7) was mounted downstream of the filler to provide pressure reduction and control. A variable area flowmeter (8) was used for the flow measurement of the air flow and installed downstream of the single stage pressure regulator. This flowmeter, also, was furnished with a needle valve for precise adjustment of the air flow. A 50 inch mercury manometer (9) mounted at the downstream side of the flowmeter was used to measure the pressure of the air flowing through the flowmeter. The temperature

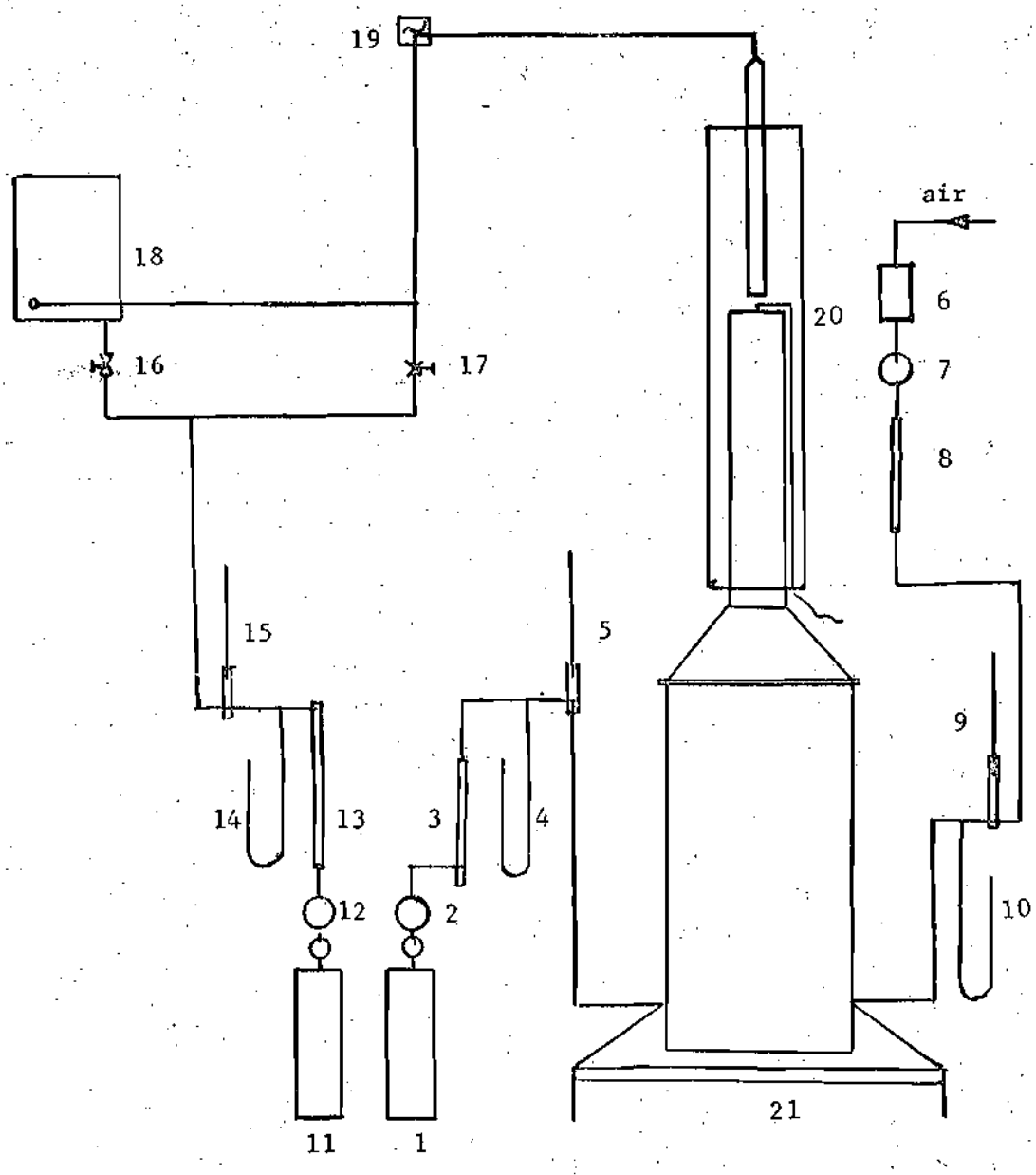

Figure 5. Schematic Diagram of Test Apparatus

Description of Figure 5

Schematic Diagram of Test Apparatus

1. Methane Tank
2. Two Stage Pressure Regulator for Methane
3. Variable Area Flowmeter for Methane
4. Water Manometer for Methane
5. Mercury Thermometer for Methane
6. Air Filter
7. Single Stage Pressure Regulator for Air
8. Variable Area Flowmeter for Air
9. Mercury Manometer for Air
10. Mercury Thermometer for Air
11. Nitrogen Cylinder
12. Two Stage Pressure Regulator for Nitrogen
13. Variable Area Flowmeter for Nitrogen
14. Mercury Manometer for Nitrogen
15. Mercury Thermometer for Nitrogen
16. & 17. Needle Valves for Nitrogen
18. Powder Feeder
19. Electric Vibrator
20. Thermocouple
21. The Burner

of the air was measured by a mercury thermometer (10 at the downstream side of the flowmeter.

Methane and air, after flowing through their respective control and measuring devices were directed to the bottom of the mixing chamber (21) to be mixed and discharged through the porous bronze plate at the mouth of the burner tube and into the reaction zone.

The particle carrier gas, nitrogen (prepurified grade), was also supplied in high pressure cylinders (11). A two stage pressure regulator (12) was mounted on the nitrogen cylinder for the pressure reduction and primary control of this gas. Flow measurement of the nitrogen gas was made through a variable area flowmeter (13) connected downstream of the nitrogen pressure regulator. This flowmeter, like those of the fuel and air, was also furnished with a needle valve in its upstream side for fine flow adjustments. A 50 inch mercury manometer (14) connected at the downstream side of the flowmeter provided the means of pressure measurement for the nitrogen. A mercury thermometer (15) was mounted in the line, downstream of the flowmeter for the nitrogen temperature measurements.

The flow of nitrogen, after passing through the flowmeter, was split into two streams. Both of these streams were controlled by needle valves (16) and (17). One stream was directed to the powder feeder to act as a carrier gas for the particles while the other stream by-passed the powder feeder. The two nitrogen streams were re-united before flowing into the particle injection tube.

The powder feed unit (18) shown in Figure 6 (Metco type 3mp powder feed unit) is a positive displacement metering device, com-

Figure 6. The Powder Feed Unit.

pletely self-contained system for delivering powders at a controlled adjustable rate. A rotating wheel with bucket-type scoops picks up an amount of powder and delivers it into a mixing chamber. The speed of the wheel can be varied through a speed control dial from 6 - 55 rpm and the amount of powder delivered is proportional to the speed of the wheel. Downstream of the meter wheel, the carrier gas picks up the powder from the mixing chamber and carries it to the delivery hose.

The rate of metal particles delivered to the reaction zone of the flat-flame burner was found to be too high when the powder feeder unit was operating with the meter wheel supplied by the manufacturer. Also, accumulation of powder which was intermittently dumped into the combustion region, occurred during the trial tests. Two modifications were incorporated into the system. The first of these consisted of replacing the meter wheel supplied by the manufacturer by a wheel with smaller bucket-type scoops. The second modification involved both the size reduction of the nitrogen-aluminum mixture line as well as the attachment of a small electric vibrator (19) upstream from the particle injection tube (see Figure 2 and 5).

The location of the powder feeder unit in relation to the injection tube was found to be critical concerning the accumulation of aluminum particles in the supply line. It became necessary to position the entire powder feeder assembly at an elevation above the injection tube and in this manner it was assured that the particles would not flow against gravity at any point. This location also made it possible to shorten the supply line. All these modifications helped to alleviate

the problems encountered initially and they provided a better operation in the feeding of aluminum powder to the burner.

The particle carrier gas flow was adjusted and monitored at the variable area flowmeter mounted directly on the 3 mp powder feed unit front panel. This flowmeter, supplied as part of the powder feed unit, was furnished with a needle valve on the downstream side of the flowmeter to enable fine flow adjustments. The flowmeter with the accompanied needle valve was located upstream of the meter wheel and mixing chamber. Therefore, it was measuring and adjusting the flow of nitrogen only.

Aluminum powder (Alcan Metal Inc., grade MD-x85-1) was the only material used in this experimental study and it provided spherical solid metal particles with an average size of 50 micrometers in diameter (58).

The flowmeters of methane, air, and nitrogen were calibrated by use of a wet-test meter connected in series with each flowmeter during the calibration runs. The calibration curves for these flowmeters at different pressures are shown on Figures C-1, 2 and 3, Appendix C.

The powder feeder flowmeter was calibrated using the flowmeter provided to measure the overall nitrogen flow rate. During these calibration runs, the by-pass line was kept completely closed and nitrogen was allowed to flow only through the powder feed unit. Figure C-5, Appendix C, shows the calibration curves for this flowmeter.

The temperatures of the hot gases generated by the flat-flame were measured by Chromel-Alumel thermocouples (20) (Leads and Northrup

Co. gage no. 28). A group of four thermocouples were supported on a rod and installed so that all of them had their thermocouple junctions at the same horizontal level. These thermocouples were used to measure the flat-flame temperature in the absence of metal particle injection. A thermocouple selector switch was installed between the thermocouples and the millivoltmeter.

When the burner was operating with the particles flow, it became apparent that the multiple thermocouple arrangement was introducing excessive disturbance in the reaction zone and the movements of the burning aluminum particles. Therefore, the thermocouples, in this case, were reduced to one. The hot gas temperatures above the burner as well as the flame temperatures were measured by this single thermocouple.

The ice-point was used as a reference temperature and a reference junction was inserted inside an ice bath for this purpose. A Leads and Northrup millivoltmeter (cat. no. 8686) was employed to measure junction emf for the thermocouples and the readings were converted to the thermometric values by appropriate conversion tables.

Experimental Procedure

It was mentioned in the previous sections that the main objective of this work was the design of a flat-flame burner incorporating an opposed flow particle injector. The burner construction and the instrumentation were discussed in some detail in the two preceding sections. Supplementing the primary objective, a qualitative experimental procedure was included to furnish some initial evaluation of the system.

A series of experiments were conducted and temperature measurements were made to provide answers to the two questions: (1) Can metal particles be ignited and burned in this experimental apparatus? and (2) How effective can this apparatus be in the study of metal particle combustion?

It may be proper to note at this point that based on the observations reported in the literature, there was some doubt in the capability of this apparatus to function properly and ignite as well as burn any metal particles. This matter will be discussed later when reporting the experimental results. The purpose of this section is to outline the procedure used in carrying out the experimental measurements.

The experimental investigation of this work was divided into three distinct phases: (a) Plain flat-flame without nitrogen or aluminum particle injection, (b) Flat-flame with only nitrogen flow from the injection tube and normal to the flame plane, (c) Flat-flame with aluminum particle and nitrogen mixture injection normal to the flame plane.

In all of the experimentation the same starting procedure was used. Air was first allowed to flow into the system by opening the valve on the main air line. The pressure was adjusted with the regulator, usually to about 40 to 50 psig. The needle valve downstream of the flowmeter was used as the main control valve. This valve was adjusted to give a desired air flow and the air was allowed to purge the system for a brief initial period. When the air flow appeared to be satisfactory, the fuel bottle was opened, the low

pressure gage on the regulator was set to approximately 7 to 15 psig and the methane flow was adjusted by the needle valve on the flowmeter to give an ignitable mixture at the reaction zone. After allowing the two gases to mix in the mixing chamber and the mixture of air and methane started moving through the burner assembly, it was ignited by an electric spark at the mouth of the burner. The spark used for the ignition of the gas mixture was generated from a hand-cranked magneto coil with a wire forming a ½ inch gap above the porous bronze matrix. The rates were then varied as needed to produce a stable flat-flame over the sintered bronze matrix plate.

During the preliminary period of experimentation, some initial flat-flame measurements were made to establish the range of air-fuel ratios. It was then observed that, as the air-fuel ratio decreased toward stoichiometric, at some region of rich mixtures a semi-diffusion flame appeared. This condition was noticeable by the formation of a conical flame region above the flat-flame and it was created by the cooling air flowing outside the burner tube, diffusing into the reaction region and producing a secondary reaction zone. The air-fuel ratio at this point was noted to be around 48 on a mass basis.

At the lean end of the air-fuel ratio the blow-off point was located. This was found to be at an air-fuel ratio of about 108. Subsequent experimentation was conducted within these two limits of air fuel ratios.

Changes in the air-fuel ratios from one valve to another were produced either by keeping the air flow constant and varying the fuel flow, or vice-versa. Whenever the air-fuel ratios were changed,

approximately five minutes were allowed for the system to reach a steady state operating condition before any measurements were made.

For the series of experiments with the plain undisturbed flat-flame, the injection tube was kept out of the system entirely. This procedure was found necessary due to the overheating of the injection tube and aluminum-nitrogen feed line. The objective of this and the other experimental phases was to establish measurements of temperatures in the reaction zone and the hot gas region at various air-fuel ratios.

In the first stage of measurements after a desired air-fuel ratio was established, the flow rates of the air and fuel were recorded from the respective flow meters along with corresponding pressures and temperatures of the gases at the meters. At the same time, a series of temperature measurements were made with the four thermocouples in the reaction and hot gas zones. The thermocouple junctions were spaced approximately 0.4 inches apart and thus provided temperature measurement capability at four places within the same horizontal plane. Temperatures at the flame edge, or at points close to the edge, were measured by rotating the thermocouple set so that the outside thermocouple would coincide with the desired location close to the edge of the flame.

For the next two major phases of experimentation the injection nozzle was placed back in the burner assembly. The distance between the matrix at the mouth of the burner and the lip of the injection nozzle was kept constant at about 0.75 inches. The injection tube exit plane was also kept parallel to the sintered bronze matrix plate.

It was considered desirable to obtain some measurements with only the nitrogen injected into the reaction zone; in the second phase of experimental measurements only nitrogen was allowed to flow through the injection tube. The line directing nitrogen to the powder feeder was kept completely closed. The flow of nitrogen was adjusted and set at different flow rates for each fixed air-fuel ratio. The range of nitrogen flow rates was selected between a minimum value that would record on the nitrogen flowmeter, and a maximum value at which the nitrogen flow from the injection tube would break down the central portion of the flat-flame and create a hole. It may be proper to mention at this point that the flow rate of nitrogen causing the breakdown in the flame varied from one air-fuel ratio to another.

For this series of tests the flow rates of the three gases were recorded along with corresponding pressures and temperatures at the flowmeter exit. During each test the four thermocouples were again used to obtain measurements of temperature in the reaction and hot gas regions. Also, at the points where the flame breakdown started, the air, fuel, and nitrogen flow rates were recorded.

Finally, in the last stage of experimentation of this work, nitrogen was allowed to flow through the powder feed unit and consequently carry aluminum particles through the injection tube into the reaction zone.

It was mentioned in the previous section that in order to eliminate excessive obstruction from the path of particles, only one thermocouple was used to record the temperatures in the burner

reaction zone. A series of temperature measurements of the hot gases (first without any particle flow and then with particles, at the same air-methane ratio and the same nitrogen flow rate) were made by this single thermocouple. Again the flow rates of the gases with corresponding pressure and temperature readings at the flowmeters were recorded for each test.

A check on the reproducibility of the measured temperatures was carried out for all three phases of experimental work. These observations will be discussed with the reporting of the results.

In this work the experimental measurements were intended to be of a qualitative nature; therefore, no attempt was made to calibrate the thermocouples and correct for the radiation effects and other heat losses. Some of the temperature values were checked by focusing an optical pyrometer to the hot thermocouple junctions. The pyrometer readings were consistently lower by 10 - 15°F than those recorded by the thermocouples on the potentiometer. This might be because of the effects of the pyrex glass chimney which was enclosing the thermocouple junction and the vision effects. Also, the consistency of the temperature measurements by an optical pyrometer to that of the thermocouple is questionable. A thermocouple is a better mean of temperature measurement than a pyrometer. The difficulty of focusing the pyrometer to the small thermocouple junction can be considered another cause of reading lower temperature than those recorded by the thermocouple.

CHAPTER III

EXPERIMENTAL RESULTS AND DISCUSSION

In the previous chapter, the experimental apparatus was discussed in detail and the objective of this work was explained. It was also mentioned earlier that some experiments were conducted to supplement the objective qualitatively and to shed light on the capability and functioning of this experimental apparatus in burning and ignition of metal particles. In addition, the presentation included some discussion on the type of investigations that were carried out, which was needed to furnish answers and guidance in the developments of techniques in studies relating to the ignition and burning of particles.

The experimental results and the operation of the designed apparatus, including some of the minor difficulties encountered, will be discussed in this chapter. The important results documented with photographs and temperature profiles including other pertinent test data will be presented in the following sections. The secondary data are presented in the appendices.

Each phase of experimentation, namely plain undisturbed flat-flame, flat-flame disturbed with nitrogen flow, and flat-flame with the aluminum-nitrogen mixture flowing on them, is duscussed and analyzed in the following sections.

Plain Undisturbed Flat-Flame

The experimental inquiries with the plain undisturbed flat-flame were performed to determine the shape of the flame and examine the maximum temperature reached by the flame at different air-fuel ratios. Also, these experiments were conducted to find the usable ranges of air-fuel ratios represented by stable flames, as well as to find the points of the flame blow-off and the appearance of the secondary flume.

Figure 7 shows a plain, undisturbed flat-flame which was stabilized on the porous bronze matrix. The experimental conditions for this and the flame photographs in Figure 10 are summarized in Table 1. The flat-flume photograph shown on Figure 7 is a typical undisturbed (by nitrogen or metal particles) flat-flame. It should be noted at this point that the actual thickness of this flame is about one-fifth of what is shown in the picture. The edge effects cause the periphery of the flame to curl upward and make the flame appear thicker when projected on the film.

The flame temperature profile of undisturbed plain flat-flames at different air-fuel ratios are shown in Figure 8. The temperature profile labeled (b) corresponds to the flame in Figure 7. These temperatures were measured only at one side of the flame, from its edge to the center. The profiles are completed in the figure for the entire flame by assuming axial symmetry at any one plane of the flame. The solid lines in Figure 8 correspond to the measured profiles while the broken lines are drawn on the basis of the symmetry assumption.

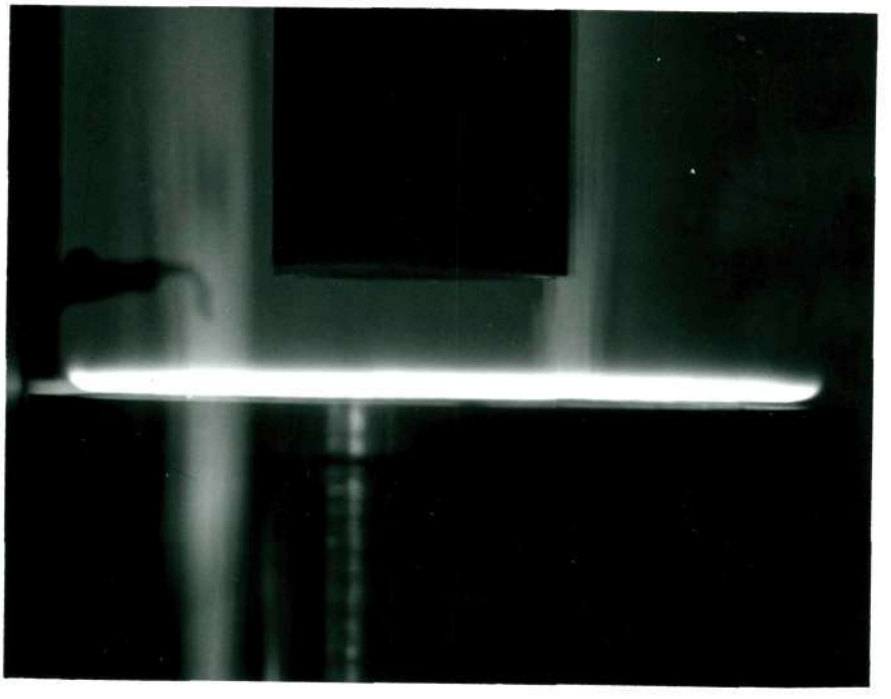

Figure 7. Plain Undisturbed Flat-Flame at AF = 93.6.

Table 1. Summary of Experimental Conditions of the Photographic Records without Particle Injection

Figure Number	AF Ratio (gm/gm)	X_{CH4} $\frac{\text{gm-mole}}{\text{gm-mole}}$	$\dot{m}_{N2}$ $\frac{\text{gm}}{\text{sec}} \times 10^3$	Maximum Temperature ^oF
7	93.6	0.092	-	1468
10	94.77	0.0833	27.3	1400

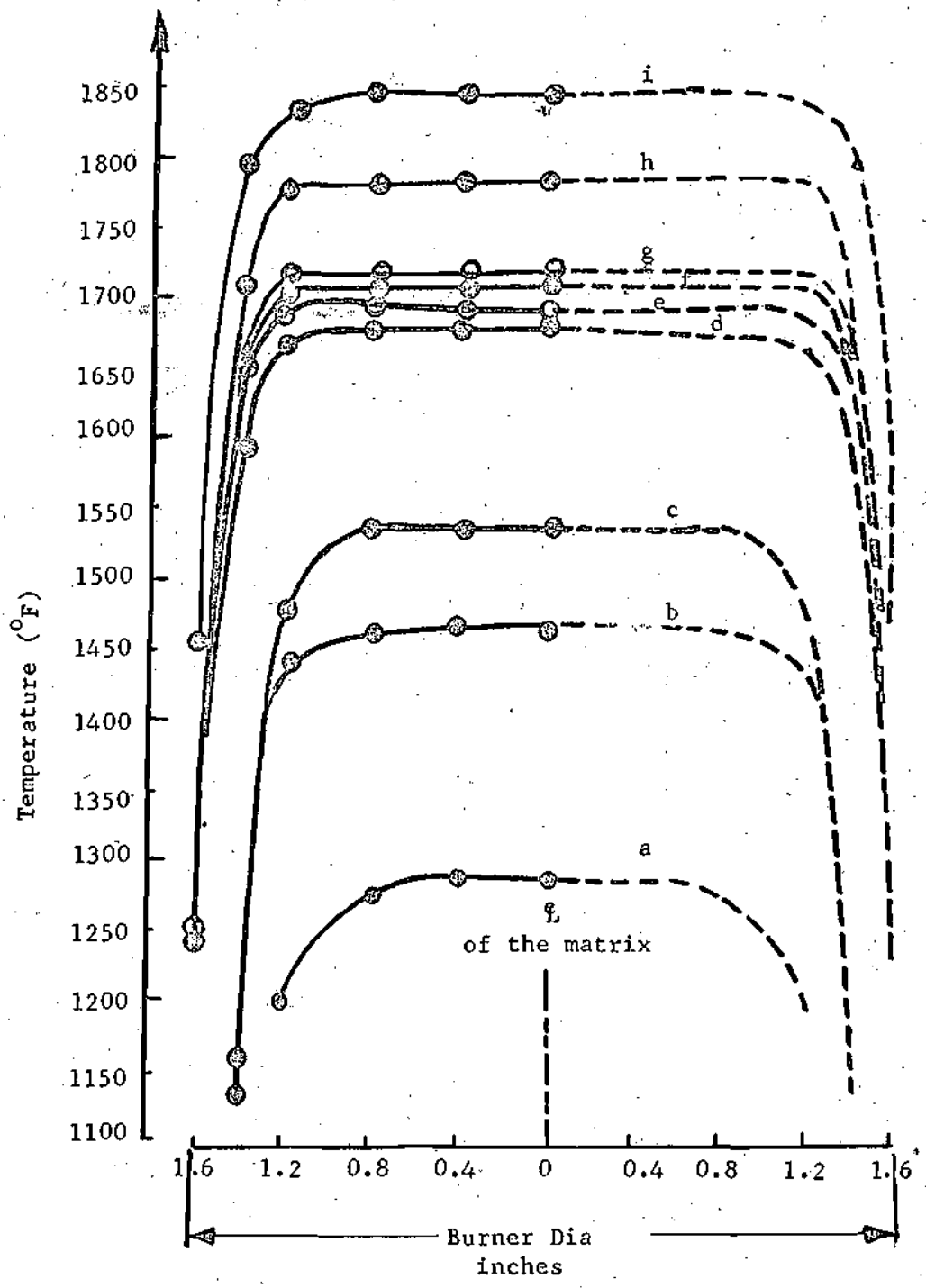

Figure 8. Flame Temperature Profiles of Flat, Plain, Undisturbed Flames; (a) AF = 108; (b) AF = 93.6; (c) AF = 87.80; (d) AF = 73.3; (e) AF = 68.25; (f) AF = 62.2; (g) AF = 53.3; (h) AF=49.3; (i) AF = 48.25.

The maximum undisturbed flat-flame temperature recorded in this burner was 1853°F, measured at the minimum possible air-fuel ratio of 48.25. This air-fuel ratio, as it was mentioned in the previous section, imposes the rich end limit of the air-fuel ratio. Beyond this limit, the secondary, semi-diffusion flame has appeared.

Examining the measured temperature profiles for the undisturbed flat-flames, it appears that the temperatures remain uniform in the main portion of the flames at a distance of about 0.4 inches from the edges. These uniformities of temperature distribution for the flames are the proof attesting to the flatness of the flames.

The experimental data of the temperature profiles shown in Figure 8 are summarized in Table A-1 in the Appendix. The maximum temperature for each of the curves increases as the air-fuel ratio decreases toward the stoichiometric value. However, the increase in temperature is not a linear function of the air-fuel ratio. This fact is apparent from Figure 9 where the variation of maximum, flat, undisturbed flame temperatures were plotted against the air-fuel ratios. The shaded areas in Figure 9 enclose the regions beyond the two limits of air-fuel ratio. The leaner flames (flames closer to the higher limit of air-fuel ratio) were more detached from the porous matrix than the rich ones. It is a well established fact that this condition is dependent both on the air-fuel ratio as well as on the velocity of the reactant gases; consequently, it is some function of the observed flame velocity. No attempt was made here to produce the necessary correlation and the results on Figure 9 are therefore reported without the benefit of a curve.

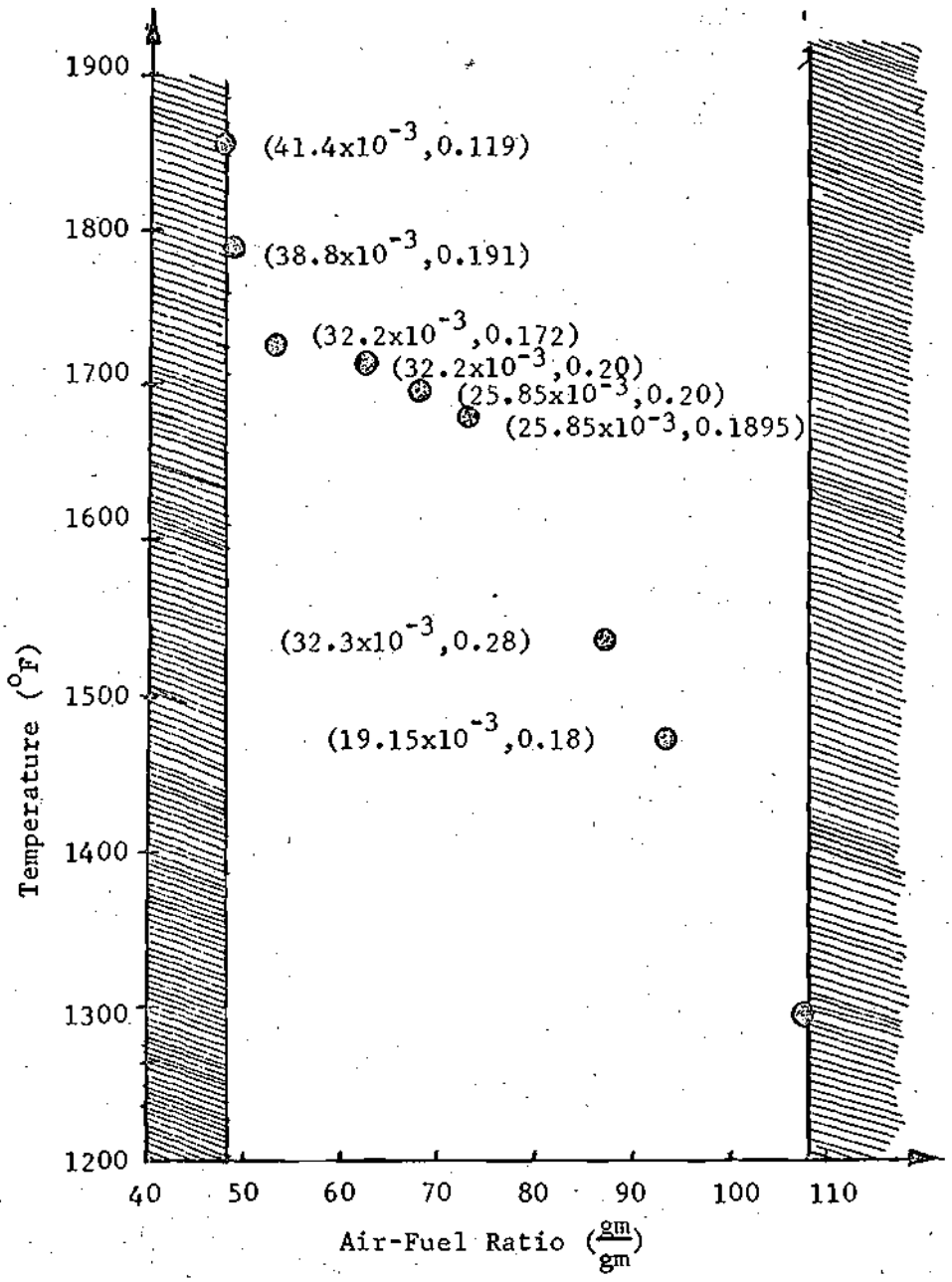

Figure 9. Maximum Plain Undisturbed Flat-Flame Temperature Variation as a Function of Air-Fuel Ratio. The First Figure in the Paranthesis Shows the Methane Flow Rate in $\frac{gm}{sec}$; the Second Figure is the Corresponding Air Flow Rate in $\frac{gm}{sec}$.

Flat-Flame Disturbed with Opposed Nitrogen Flow

Some preliminary study of the nitrogen effects on flat flames was the second objective of the experimental work. It was aimed to record the temperature reduction in the reaction zone, observe any changes in the shape of the flame due to nitrogen impingement, and record the ranges of nitrogen flow within which the flat-flame is not severely disturbed.

Figure 10 shows a flat-flame with nitrogen flow from the opposite direction and impinging on the flame. This flame just like the undisturbed flame, appears much thicker on the photograph. The exaggeration is even more severe in this case. The flame was leaner in reactant composition compared to the plain flame in Figure 7, and at the same time, it was more detached from the burner bronze matrix.

Temperature measurements of the flame in the presence of nitrogen flow were made at three positions within the flame at the same horizontal plane and at varying nitrogen flow rates. The positions selected were near the outer edge of the flame, directly under the edge of the injection nozzle, and at the center of the flame. Figures 11, 12, and 13 represents the temperature profiles as a function of the nitrogen flow rate for the air-fuel ratios of 93.6, 68.25, and 48.25 respectively. Temperature profiles for other air-fuel ratios are included in Appendix A (Figures A-1, A-2, A-3, and A-4).

The cooling effects of nitrogen on the flames can be seen in the temperature profile curves. The rate of temperature reduction with nitrogen flow was faster at the center and its vicinity of the flame than in the regions outside of the injection nozzle mouth. The tempera-

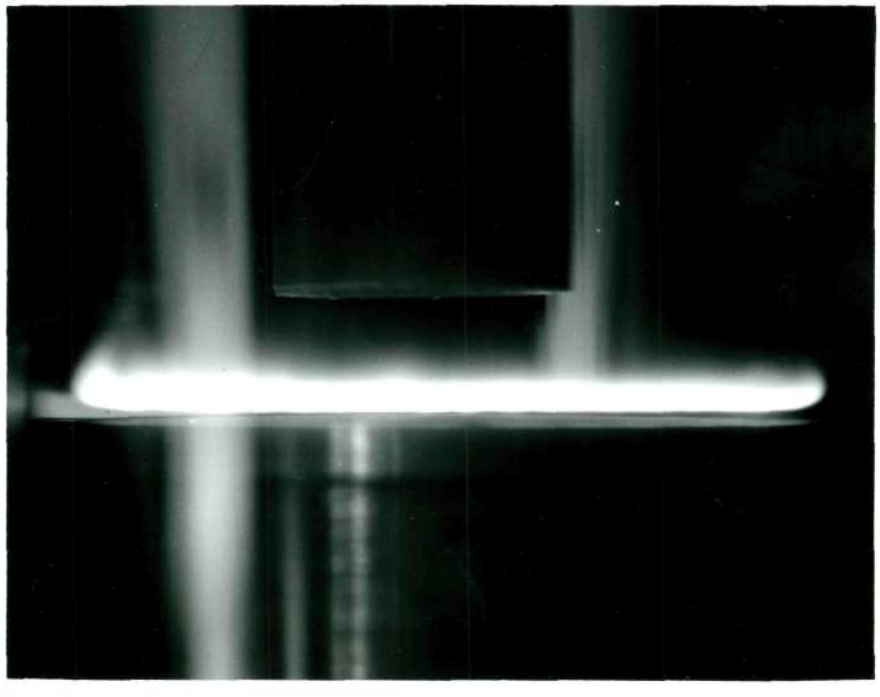

Figure 10. Flat-Flame with Opposed Nitrogen Flow at AF = 94.77 and $\dot{m}_{N2} = 27.3 \times 10^{-3} \frac{gm}{sec}$.

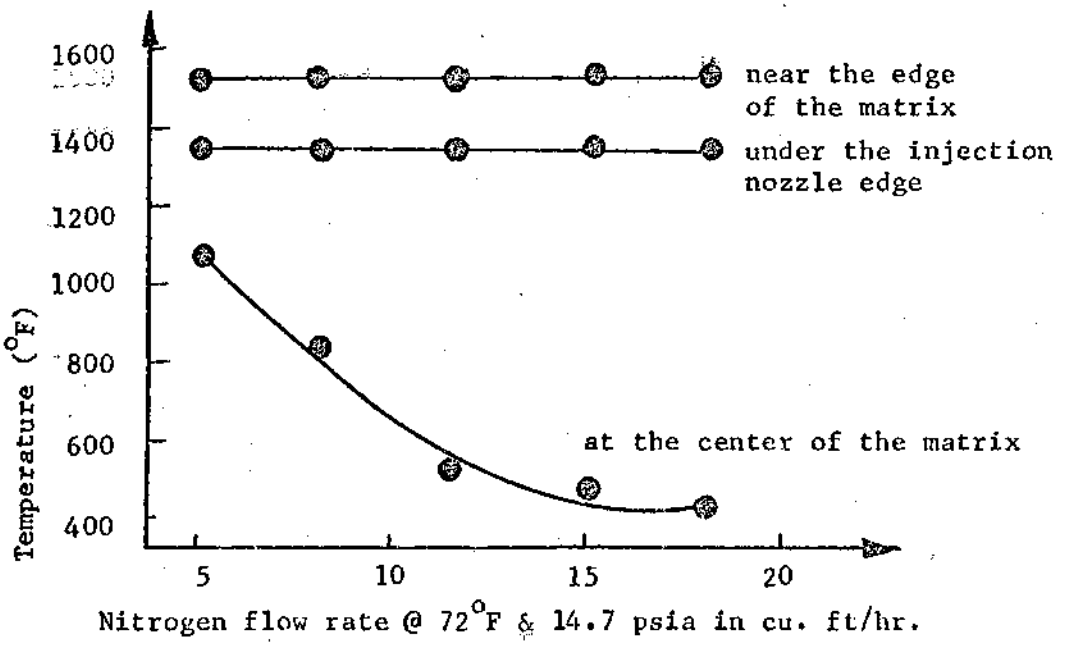

Figure 11. Flat-Flame Temperature Variation with Opposed Nitrogen Flow; AF = 93.6.

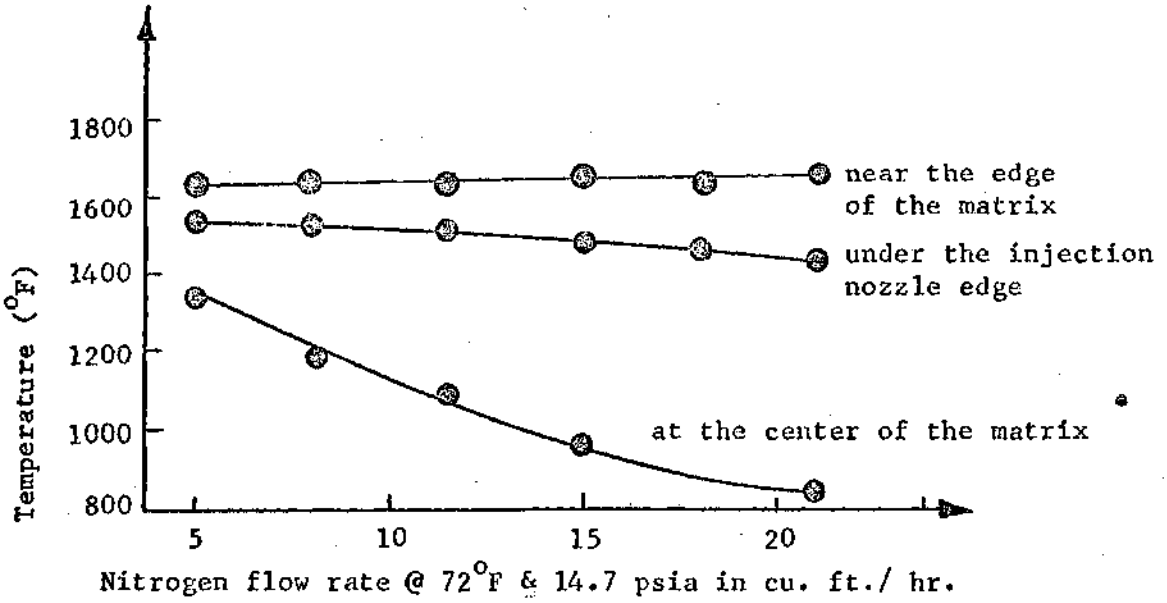

Figure 12. Flat-Flame Temperature Variation with Opposed Nitrogen Flow; AF = 68.25.

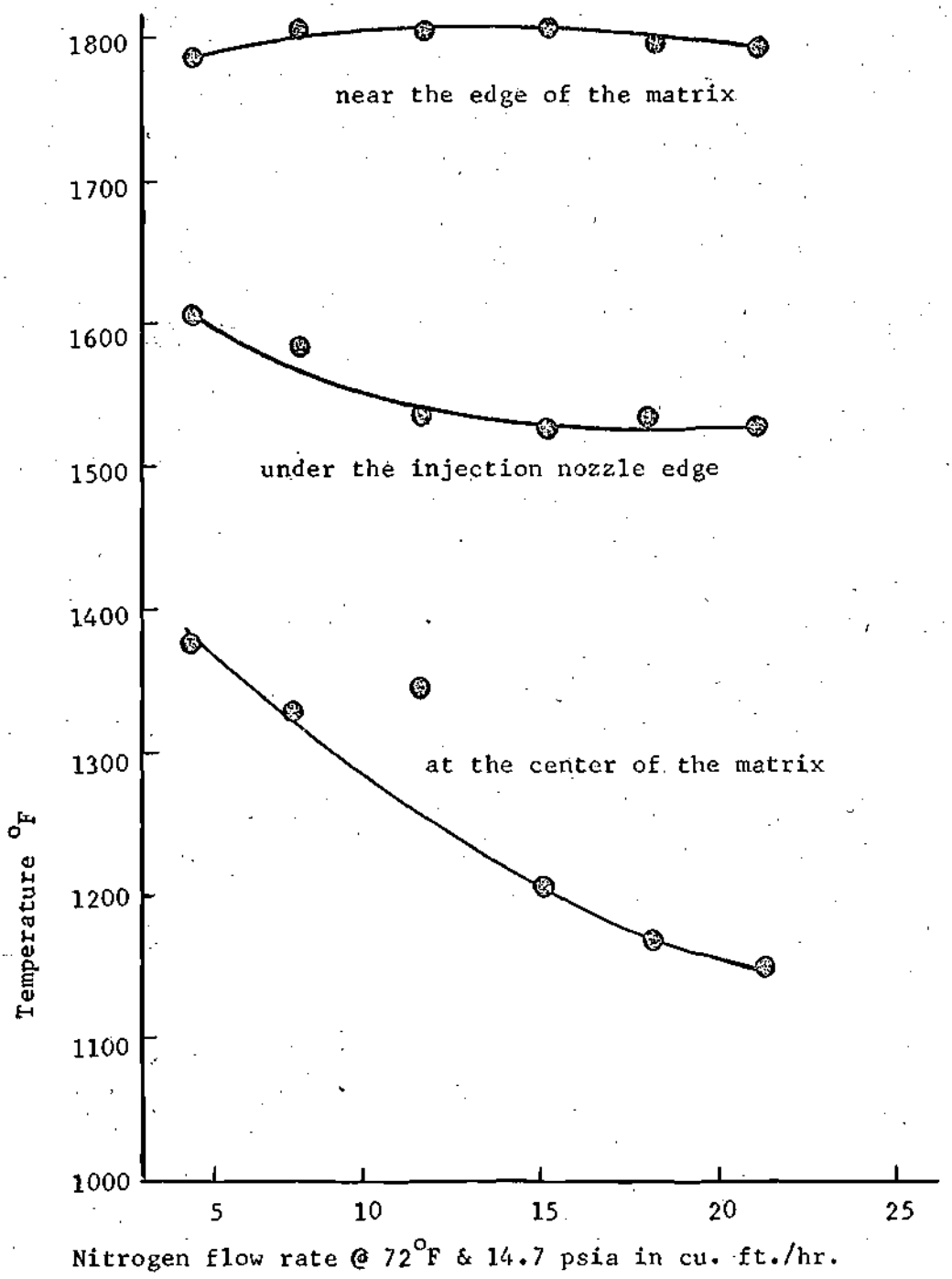

Figure 13. Flat-Flame Temperature Variation with Opposed Nitrogen Flow; AF = 48.25.

tures near the outer edge of the flame remained close to the values measured with the undisturbed flames. For each fixed value of nitrogen flow, the flame temperature was a maximum in this region of the flame and a minimum at the center. This is a fact which is clearly evident from Figures 14 and 15 where plots of the temperature variation as a function of distance at the flame plane and at a constant nitrogen flow rate are shown.

It is also apparent that the variation in nitrogen flow rate, for all air-fuel ratios had practically no effect on the outer edge of the flame where the temperature measurements indicate a uniform value to exist. It is clear, therefore, that nitrogen flow direction reverses completely after impinging on the flame; and it adheres, as it mixes with the combustion products, close to the outer edge of the injection tube. The reversal of the flow direction is due to the higher velocity of the gases (combustion products gas) in the reaction zone. This fact, which is aupported by the temperature profiles shown in Figures 11, 12, 13, A-1, A-2, A-3, and A-4, is also documented by photographic evidence observed when particles were injected to the flame. Figures 17, 18, 19, 20, 21 which will be presented and discussed fully in the next section, show the flow direction of metal particles and the nitrogen after striking the flame.

Temperatures were also measured at a plane parallel to the flat-flame and 1.6 inches above it. The profile is shown in Figure 16. The fact that nitrogen adheres close to the injection tube is evidenced by the low temperature near the wall of the tube.

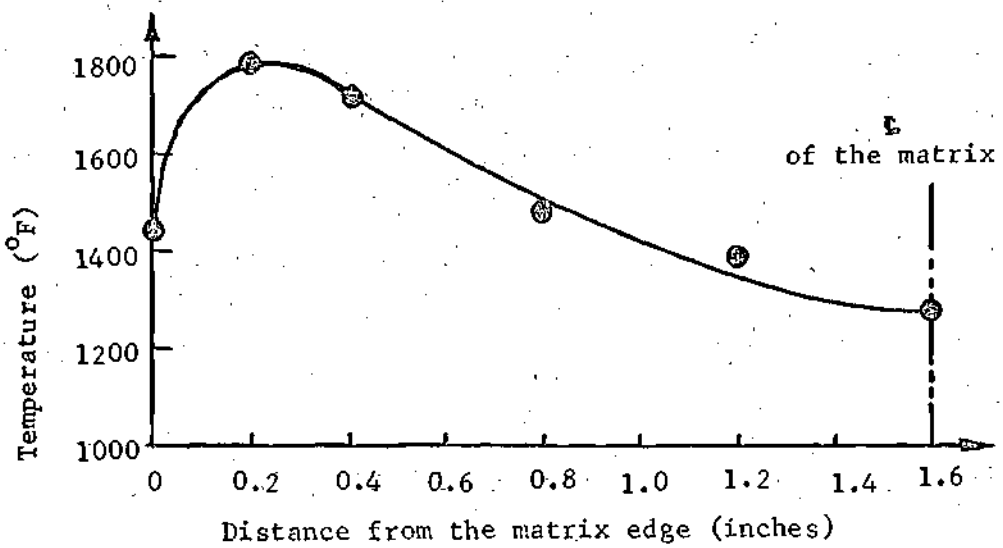

Figure 14. Flame Temperature Profile with Opposed Nitrogen Flow; AF = 52.2, $\dot{m}_{n_2} = 45.7 \times 10^{-3} \frac{gm}{sec}$.

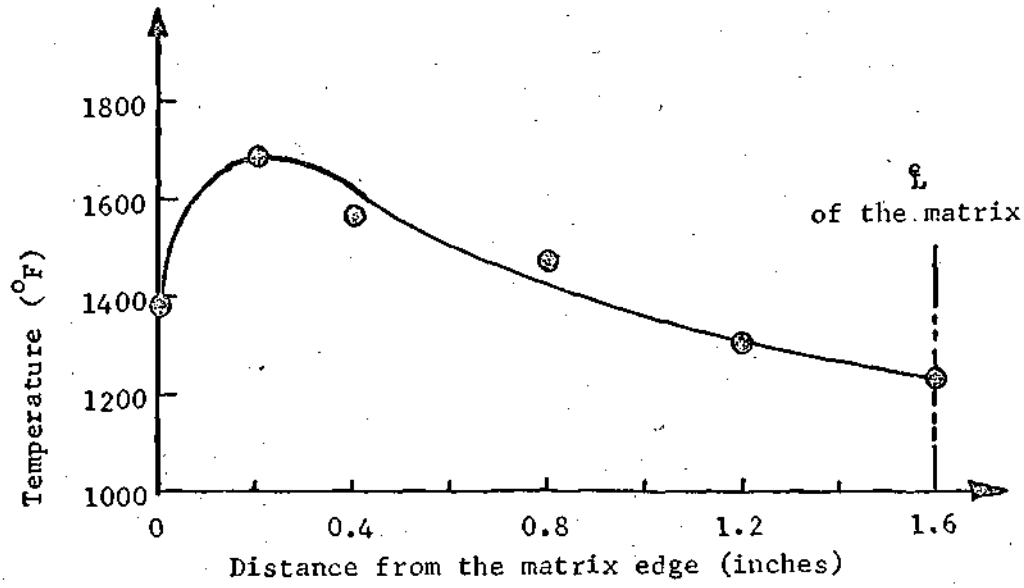

Figure 15. Flame Temperature Profile with Opposed Nitrogen Flow; AF = 64, $\dot{m}_{n_2} = 73.1 \times 10^{-3} \frac{gm}{sec}$.

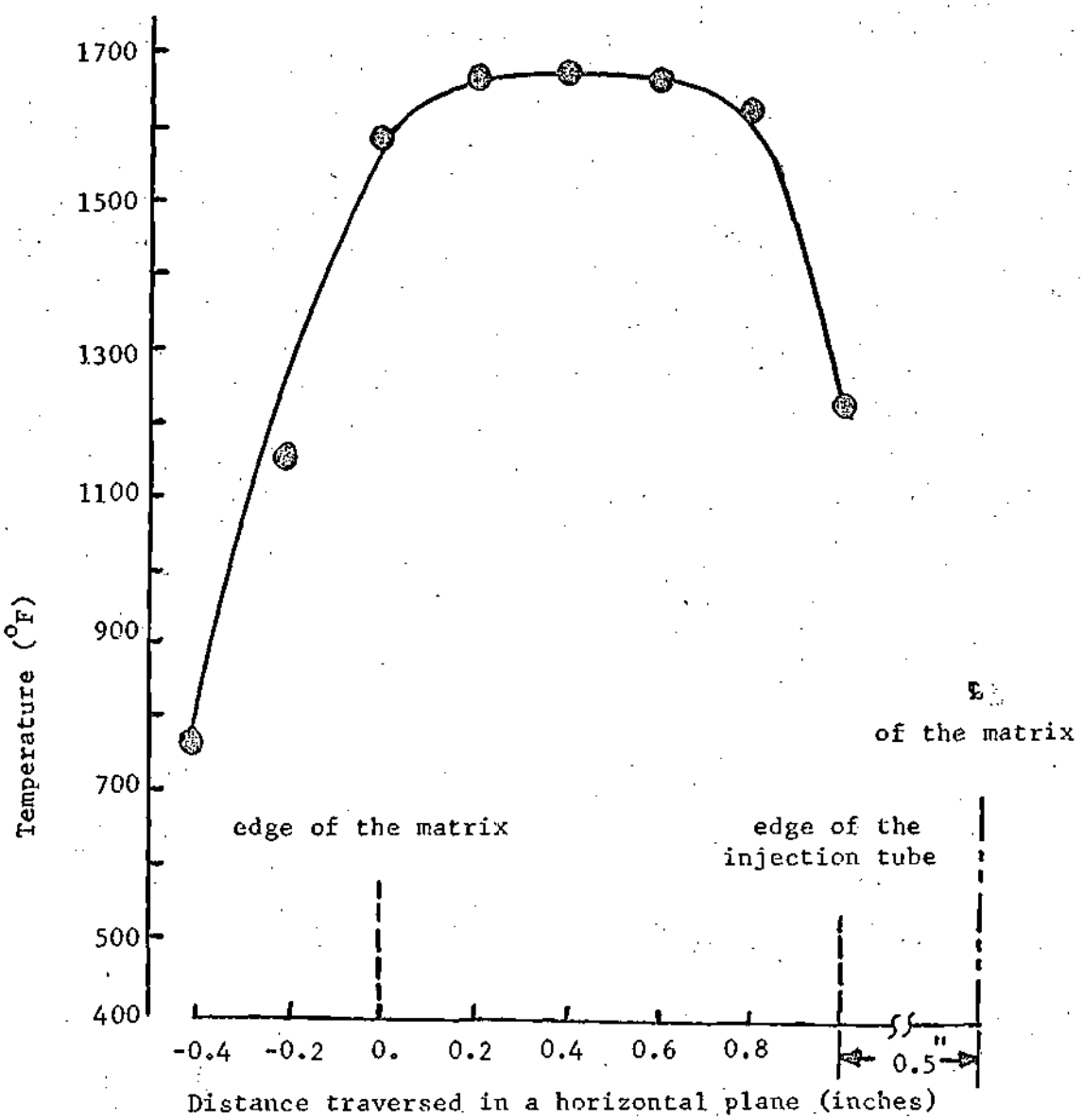

Figure 16. Hot Gas Temperature Profile in a Plane Parallel to the Flat-Flame and 1.6 Inches Above the Flame; AF = 48.25, $\dot{m}_{N_2} = 73.1 \times 10^{-3} \frac{gm}{sec}$.

Naturally this temperature is also lowered due to heat exchange through the wall with the cooler nitrogen flowing inside the injection tube. Another point of interest is the fact that the temperature profile has become flat in the region between the edge of the tube and the projected edge of the matrix.

For flat-flames in the presence of nitrogen flow, only the lean air-fuel ratio limit was affected when compared with the undisturbed flat-flames. The flames were extinguished at a lower air-fuel ratio when nitrogen flow was present. For example when the nitrogen flow rate was $45.7 \times 10^{-3} \frac{gm}{sec}$, the extinction air-fuel ratio was observed to be approximately 100 compared to 108 of undisturbed flat-flame. However it appeared that the rich limit of air-fuel ratio remained approximately the same as those observed for the undisturbed plain flat-flame.

Flat-Flame with Nitrogen-Particle Opposed Flow

One of the main objectives of the experimental part of this investigation was to learn whether or not it is possible to ignite and burn metal particles in the designed experimental apparatus. Analysis of the results presented in a series of temperature profiles at the presence and absence of the metal particles for different reactant gas compositions at atmospheric pressure, and different rates of aluminum particle flow, as well as nitrogen flow, yield evidence that it is possible to ignite and burn small aluminum metal particles, using the designed flat-flame burner with the opposed particle jet configuration.

Figures 17, 18, 19, 20 and 21 show the paths traced by reacting

Figure 17. Aluminum Particles Burning with Flat-Flame Ignition--
Air-Methane Ratio = 91.5 (Plus x, f 8, 15 sec.).

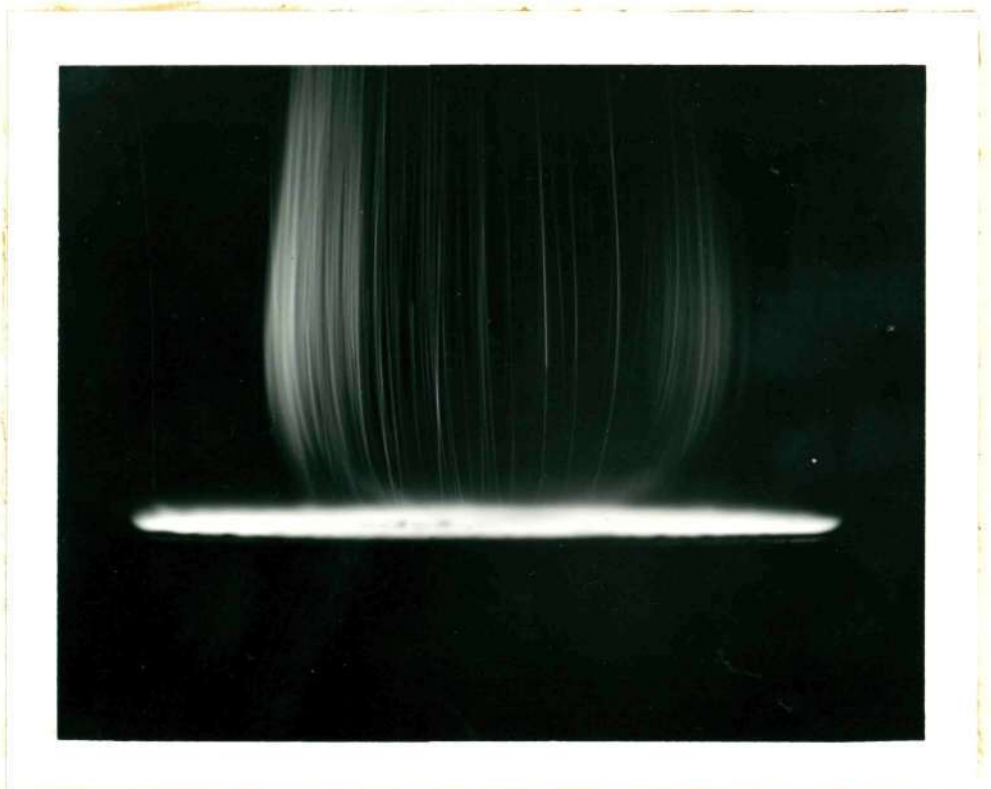

Figure 18. Aluminum Particles Burning with Flat-Flame Ignition--Air-Methane Ratio = 79 (Tri-x, Ortho, f 8, ½ sec.).

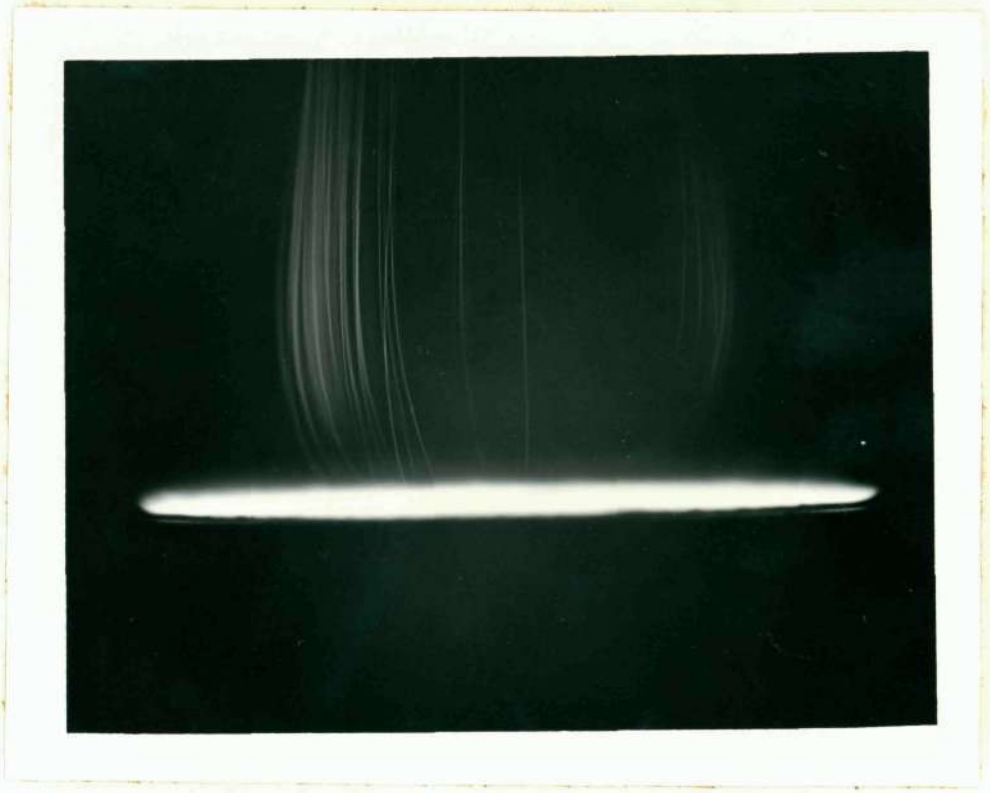

Figure 19. Aluminum Particles Burning with Flat-Flame Ignition--Air-Methane Ratio = 77.5 (Tri-x Ortho, f 8, ½ sec.).

Figure 20. Aluminum Particles Burning with Flat-Flame Ignition--Air-Methane Ratio 91.5 (Plus x, f 8, 30 sec.).

Figure 21. Aluminum Particles Burning with Flat-Flame Ignition--Air-Methane Ratio = 91.5 (Plus x, f 8, 60 sec.).

aluminum particles injected into the flat-flame. The flow rates, as well as air-methane ratio and the maximum temperature for these flames, are presented in Table 2. The conditions of the flat-flames with and without nitrogen and nitrogen-aluminum mixtures have been included for convenience and comparison.

As it was mentioned in the previous chapter, there was some question with regard to the ignition of metal particles in the flames achieved by the designed burner. The uncertainty was the result of the knowledge that the temperatures produced by the methane-air flat-flames never reach the aluminum ignition temperature requirements reported in the literature.

A review of the literature (7,9,10,11,15,40) reveals that the ignition temperature observed for aluminum particles or aluminum wires burning in an oxygen-containing atmosphere is about 2300°k. In other words, it indicates that aluminum will ignite when the hot gas temperature reaches a value of about 3680°F. At the same time, in the burning of aluminum wires, a glowing temperature of 2025°k (3186°F) was reported (15). The ignition temperature of aluminum particles has also been studied theoretically and measured experimentally in a system where small aluminum particles (30 - 50 micrometers in diameter) were injected into a hot medium produced by propane-air flat-flame (10,11). The particles were injected axially into the stream of hot gases flowing in the same direction.

In Figures 8 and 9, where temperatures for the plain air-methane flat-flame were reported, the maximum measured temperature achieved is shown to be 1853°F.

Table 2. Summary of Experimental Conditions of the Photographic Records

Figure Number	AF[1] $(\frac{gm}{gm})$	X_{CH4} $\frac{gm\text{-}mole}{gm\text{-}mole}$	$\dot{m}_{N2}$[2] $(\frac{gm}{sec})x10^3$	$\dot{m}_{Al}$ $(\frac{gm}{sec})x10^2$	$\dot{m}_{N2}$ Total $(\frac{gm}{sec})x10^3$	Maximum Temperature (°F)
7	93.6	0.092				1468
10	94.77	0.0833			27.3	1400
17	91.5	0.0925	17.27	2.15*	27.3	1790
18	79.0	0.098	31.80	1.15	73.1	1780
19	77.5	0.100	28.2	1.10	45.7	1750
20	91.5	0.0925	27.3	0.98	45.7	1710
21	91.5	0.0925	17.27	0.0265**	27.3	1650

(1) AF = Air-Methane Ratio.

(2) $\dot{m}_{N2}$ = Mass flow rate of nitrogen through the powder feeder.

* This value obtained with the meter wheel of the powder feeder rotating.

** This is an approximate value obtained by a count of particles.

A close examination of the photographs with the particles reveals the path traced by the particles as they move away from the flame. The photograph in Figure 21 is especially significant since it records more clearly the paths of the individual particles. For this particular test, less than 12 particles per second were injected into the flame. Some of the particles, as it is evidenced from this photograph, and other experimental observations while they are reacting and travelling in the same direction as the stream-lined flow of methane-air combustion products, are demonstrating irregularities in their motion. These irregularities in the motion of the particles can be due to the particle fragmentation and spinning reported in the literature and observed when aluminum particles burned in the presence of water vapor, nitrogen, or any impurities in the medium (33, 34, 40). The higher densities of aluminum particle flow, as recorded in other photographs, makes it difficult to reveal this type of phenomena in the motion of the particles if they are present.

A comparison of the experimental measurement of the temperatures in the hot gaseous medium indicates a significant increase when the metal particles were injected into the medium. Figures 22 and 23 are temperature profiles for a series of tests where the air-methane ratio, mole fraction of methane, and the nitrogen flow rates were kept constant. The curves labeled (a) in both figures show temperature profiles when no aluminum particles were present in the injected nitrogen, while the curves labeled (b) in these figures are the temperature profiles when aluminum particles were injected with the nitrogen carrier gas. The profiles in Figure 22 have been traversed in the horizontal flat-flame

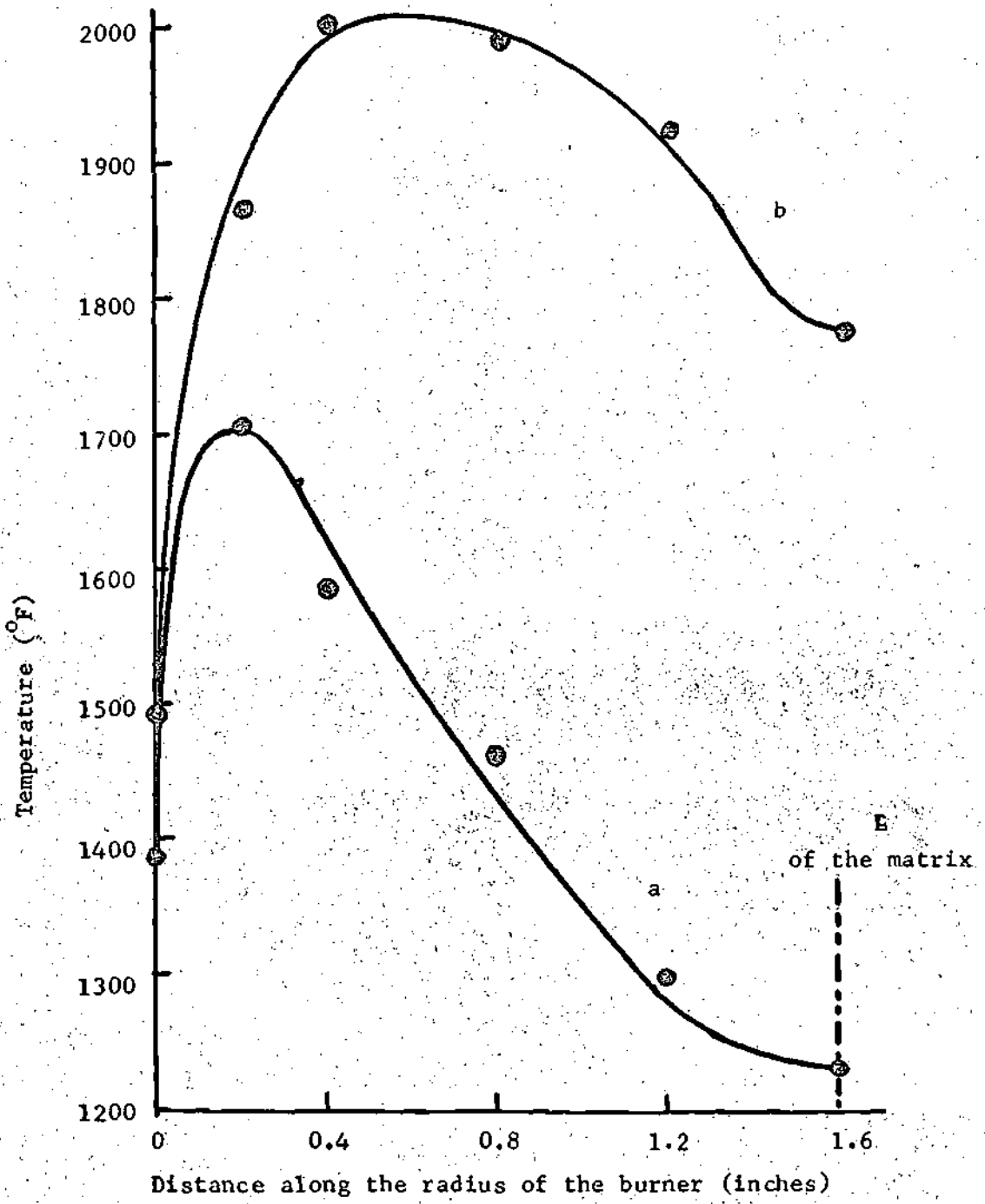

Figure 22. Flat-Flame Temperature Profile with Nitrogen and Nitrogen-Particle Flow; (a) $\dot{m}_{N2} = 73.1 \times 10^{-3} \frac{gm}{sec}$; (b) $\dot{m}_{N2} = 73.1 \times 10^{-3} \frac{gm}{sec}$, $\dot{m}_{Al} = 2.5 \times 10^{-2} \frac{gm}{sec}$, $\dot{m}_{N2}$ (through the powder feeder) $= 36.5 \times 10^{-3} \frac{gm}{sec}$.

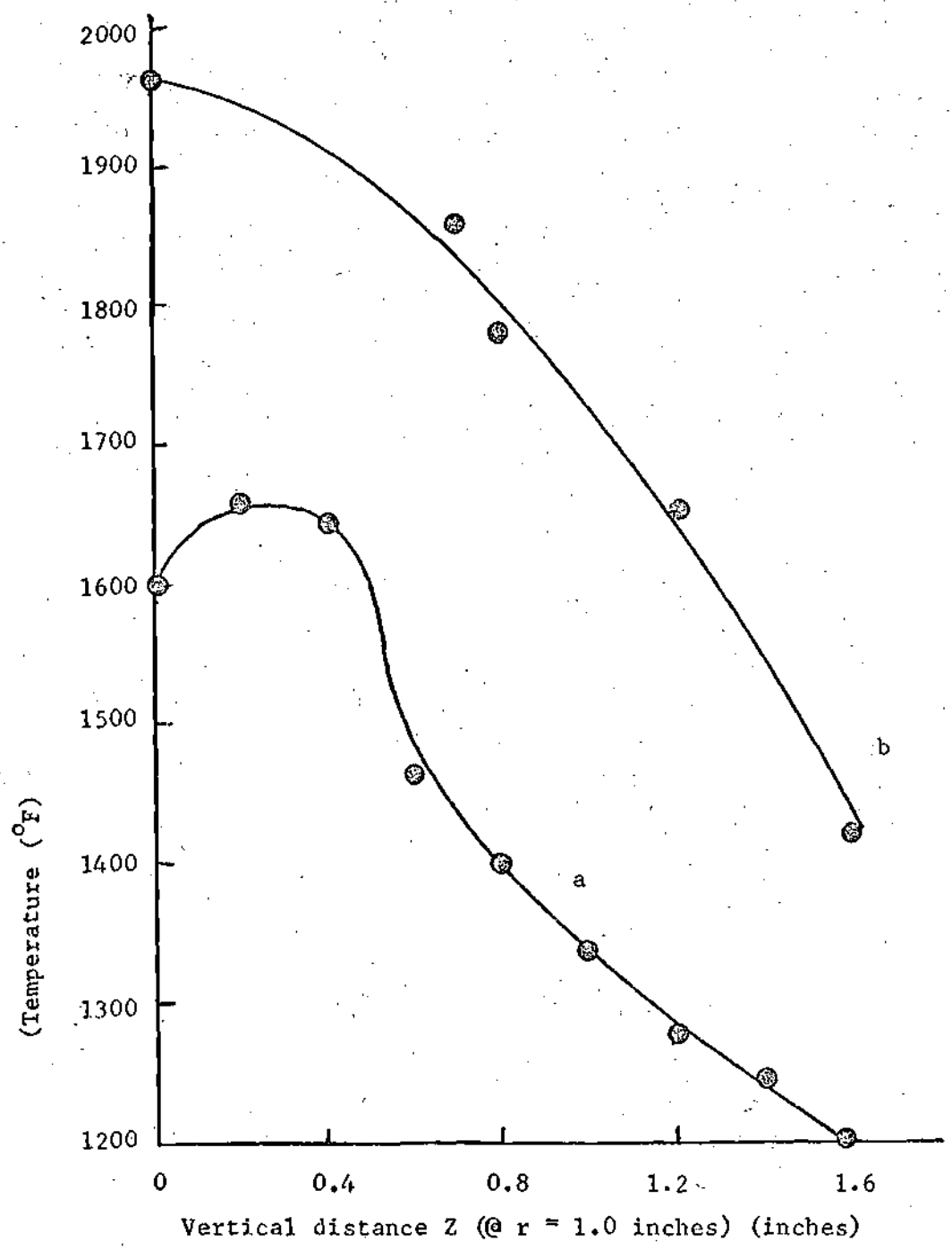

Figure 23. Hot Gas Temperature with Nitrogen and Nitrogen-Particle Flow Nozzle; (a) AF = 52.2, $\dot{m}_{N2}$ = 73.1 x 10^{-3} $\frac{gm}{sec}$; (b) $\dot{m}_{N2}$ = 73.1 x 10^{-3} $\frac{gm}{sec}$, $\dot{m}_{Al}$ = 2.5 x 10^{-2} $\frac{gm}{sec}$, $\dot{m}_{N2}$ (through the powder feeder) = 36.5 x 10^{-3} $\frac{gm}{sec}$.

plane. For the measurement of the temperatures presented in Figure 23, the thermocouple junction was placed at the points of constant radial distance, slightly outside the projection of the injection tube. Starting with the flame plane as the reference point, the thermocouple was moved in a vertical direction away from the flat-flame while recording the medium temperatures. The same procedure was used for the measurement of temperatures in the presence of particles.

The increase of the flame temperature and the temperature of the flowing gases, as they are evidenced from these profiles, are naturally due to the additional heat release from the reacting aluminum particles.

The results of this preliminary experimental investigation indicate that, it is possible to ignite and burn aluminum metal particles in the flames produced by this type of burner configuration in much lower temperatures than those reported in the literature. A more methodical evaluation of the system is indeed needed and this will be discussed later.

The item that distinguishes our experimental apparatus from those previously used by other investigators in the aluminum particle combustion studies is the method of introduction of the particles into the reaction zone. The aluminum particles suspended in the nitrogen carrier gas flow through the one foot long tube, and they are injected axially from the opposite side against the flow of hot gases. By introducing particles in a counterflow arrangement through the particle injector nozzle, enough time is allowed for the particles, while travelling in a bounded flow region, to be preheated

before they impinge into the flame. It is probable that this preheating of nitrogen and the particles from the surrounding hot gases produces sufficient rise in the particle temperature to provide ignition when they enter the flame, and a self-sustained burning condition.

The particular design selected in this experimental apparatus for the introduction of the particles into the flame produces one difficulty. When the particle flow rate was increased substantially, a considerable quantity of the metal particles and as they burned their solid oxides collected on the porous bronze matrix. This collection of particles on the matrix had the effect of disturbing the aerodynamic flow conditions of the hot gases, and at the same time, increased the radiation due to the collected glowing material. However, it was possible to reduce this problem considerably by lowering the particle flow rate. Examples of both cases are presented in the photographs. Figure 17 shows the collected particles on the matrix while Figure 21 shows no collection of particles at all.

In most of the experiments carried out in this work, the collection of particles on the matrix was avoided. This condition was achieved by turning off the meter wheel in the powder feeder and maintaining low particle flow rates. All of the photographic records, with the exception of Figure 16, were obtained under these conditions. One of the most favorable and properly controlled operations is shown in Figure 21. A comparison of the two extreme cases in the photographic records reveals that, in Figure 16, 0.0215 $\frac{gm}{sec}$ of aluminum particles were fed into the reaction zone when the meter wheel was rotating, while in the case of Figure 21, the meter

wheel was turned off and the aluminum particle flow rate was reduced drastically by two orders of magnitude to about 0.000265 $\frac{gm}{sec}$. In both of these cases the same rate of nitrogen flow passed through the powder feeder.

One additional observation that should be reported at this point relates to the material accumulation on the matrix. Regardless of the quantity of the accumulated residue, no melting of the aluminum or aluminum oxide could be observed on a macroscopic scale. The residue generally remained as a powdery substance and it was possible to brush off all the material from the top of the matrix without any portion of it attaching to the matrix, even when the flat-flame was present.

In observing the tracks produced by reacting particles, it appears that the majority of them originate in the flat-flame and project away from the flame. In some instances, the particles seem to ignite when they flow away from the flame after striking the flat-flame plane. This condition can be seen from brighter sharp streaks of the particles at some distance from the flame, when flowing in the same direction as the hot gases. Examples of this condition can be found in Figures 18 and 19.

A check on the reproducibility of the temperatures measured during all three phases of the investigation was made. It was found that in the first phase of experimentation, dealing with the plain undisturbed flat-flame, the measured temperatures were reproducible with 10 - 15°F. The other experiments were reproducible within 15 per cent of the measured temperature. The errors involved appear

to increase when the flat-flame is disturbed with the nitrogen and particle flows. This increase in the error must be related to some effects resulting from the nitrogen and particle flow on the flame and the hot flowing gases. The lack of a method for the precise location of the thermocouples can also be viewed as an additional source of error.

CHAPTER IV

CONCLUSIONS AND RECOMMENDATIONS

The objective of this work was to develop new techniques in the burning of particles. The experimental apparatus consisting of a premised flat-flame burner with a counter flow particle injector was designed and its applicability in this field was tested. The results of these tests were presented and discussed in the previous chapter.

The first task was to obtain flat-flames. The photographic records in Figure 7 and 10 and the temperature profiles of Figure 8 support the existence of the flat-flames. The second stage of experimentation was aimed to investigate the effects of an axially opposed flow nitrogen stream on these flames. With the aid of temperature measurements, Figures 11 through 15 and Figures A-1 through A-4 in Appendix A, the cooling effects of the nitrogen on these flames were observed. It was also found that flat-flames can resist the flow of nitrogen up to some limit and then the central portion of the flame breaks away. The strength of each flame to resist this nitrogen flow was found to be a function of the mixture rationof the reactant gases as well as the velocity of nitrogen flow. Other effects caused by nitrogen flow impinging normal to flat-flame plane were the lowering of the lean extinction limit of the flames and the establishment of a peak temperature close to the outer

edge of the flames. However, these peaks became flatter at some distance above the flame plane as indicated in Figure 16.

The third objective, which was a constituent part of this investigation, was directed towards a study which will reveal some information in the behavior of particles when injected with a carrier gas in an axially opposed flow stream on the flat-flame. The aluminum metal particles that were used in this case ignited and burned in these flames. The ignition of these small metal particles was observed and documented with still photographs and the measured temperature profiles shown in Figure 17 through 23.

Most of the aluminum particles appeared to ignite when they interfered with the flat-flame, and their burning started in the flat-flame zone. Some of the particles, on the other hand, were ignited and burned in the hot flowing gases shortly after they were propelled away from the flat-flame. The existence of a reactive process with the aluminum was evidenced through the increase in the temperature everywhere in the flowing gaseous medium.

The use of the counter flow system for the injection of particles into a premixed flat-flame can possibly be the main factor with regards to the ability to ignite and burn metal particles in a medium of lower temperature than those observed by the other investigators. It is very much apparent that further investigation is needed to study this effect and the capability in igniting aluminum particles at these low temperatures.

The results of this preliminary research show that this system of flat-flame burner with an opposed flow particle injector can be

used in the study of metal particle combustion. The system is found to have the potential of providing enough heat and high temperatures to ignite and burn aluminum metal particles. However, some modifications of the system are required for proper control of certain parameters and effects.

The present design allowed ambient air to enter the system, cool the burner, and mix with the combustion products as it moved up through the pyrex glass chimney. This air, however, provided an additional source of oxygen supply for the periphery of the reaction zone and imposed a limit in the use of the entire range of air-methane mixtures that establish a stable flame. It was not possible, therefore, to use lower air-methane ratios without the existence of a secondary flame. A review of literature in the combustion of aluminum particles reveals that nitrogen participates in the combustion process, which in turn has an effect on the modes of combustion of this metal. In addition, moisture content in the air has also been observed to have some influence in the combustion process of the metal particles. Therefore, the substitution of an inert gas to flow between the pyrex glass chimney and the burner is recommended for future experimentation. Reducing the amount of nitrogen from the reaction zone may result in a better control and understanding of the combustion characteristics of aluminum particles. Consequently, the commutation of another gas, such as argon, as the particle carrier gas should be considered and the comparative effects studied. Moisture content of air should also be controlled or eliminated with the use of moisture removal filters. The water vapor in the reaction zone will be limited only to the

quantity produced from the methane reaction.

The measurement of temperatures should be considered to include thermocouple calibrations and corrections for radiation and other heat losses. Optical and spectrographic methods of temperature measurements should be considered as supplementary or alternate methods in future studies on the ignition and burning of particles.

Finally, the particle flow rate control should be improved to allow proper adjustments at low particle flow rates. Modifications in the part of the system which include the powder feeder will be necessary to enable the injection and accurate control of particles at low rates. It is expected that it will be easier to assess the information regarding the burning characteristics of the metal particles and to study the effects of various parameters when the particles injected are kept at a low rate.

APPENDICES

APPENDIX A

TEMPERATURE DATA AND PROFILES

The tables in this appendix include tests data of temperature measurements for (1) the undisturbed plain flat-flame, (2) flat-flames with only nitrogen flow, and (3) flat-flames with nitrogen-aluminum mixture injection.

Table A-1. Undisturbed Plain Flat-Flame Temperature Variation Across the Flame at Different Air-Fuel Ratios (Figure 8)

r(1) inches	AF $\frac{gm}{gm}$	X_{CH4} $\frac{gm\text{-}mole}{gm\text{-}mole}$	Flame Temperature °F	AF $\frac{gm}{gm}$	X_{CH4} $\frac{gm\text{-}mole}{gm\text{-}mole}$	Flame Temperature °F
	108	0.074		93.6	0.092	
1.6			572			698
1.4			824			1137
1.2			1201			1440
0.8			1280			1463
0.4			1290			1465
0			1286			1468
	87.80	0.0933		73.3	0.104	
1.6			1074			1244
1.4			1160			1591
1.2			1480			1672
0.8			1538			1675
0.4			1529			1678
0			1535			1681
	68.25	0.112		62.2	0.1195	
1.6			1247			1241
1.4			1643			1670
1.2			1690			1710
0.8			1696			1714
0.4			1688			1712
0			1694			1714
	53.3	0.140		49.3	0.148	
1.6			1233			1331
1.4			1663			1731
1.2			1722			1786
0.8			1714			1778
0.4			1723			1785
0			1721			1789
	48.25	0.1485				
1.6			1455			
1.4			1796			
1.2			1837			
0.8			1845			
0.4			1853			
0			1850			

(1) r = radial distance across the flame

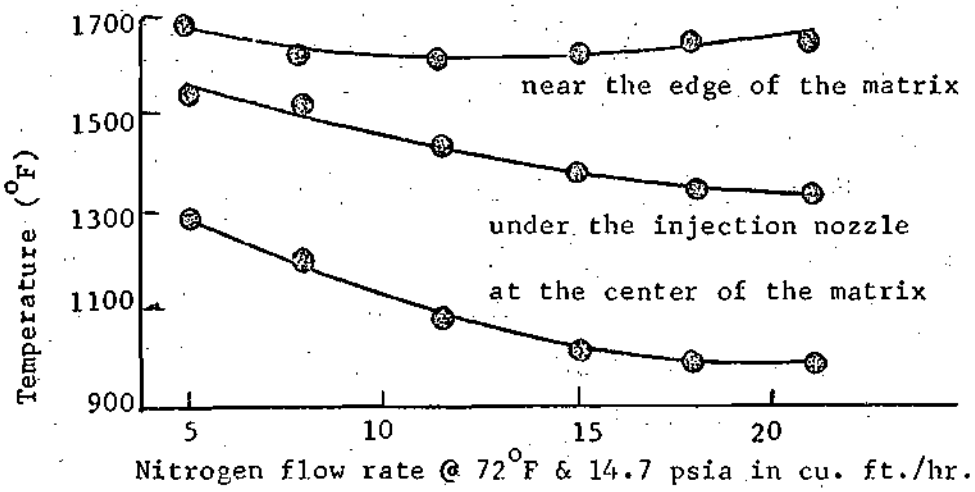

Figure A-1. Flat-Flame Temperature Variation with Opposed Nitrogen Flow; AF = 62.2.

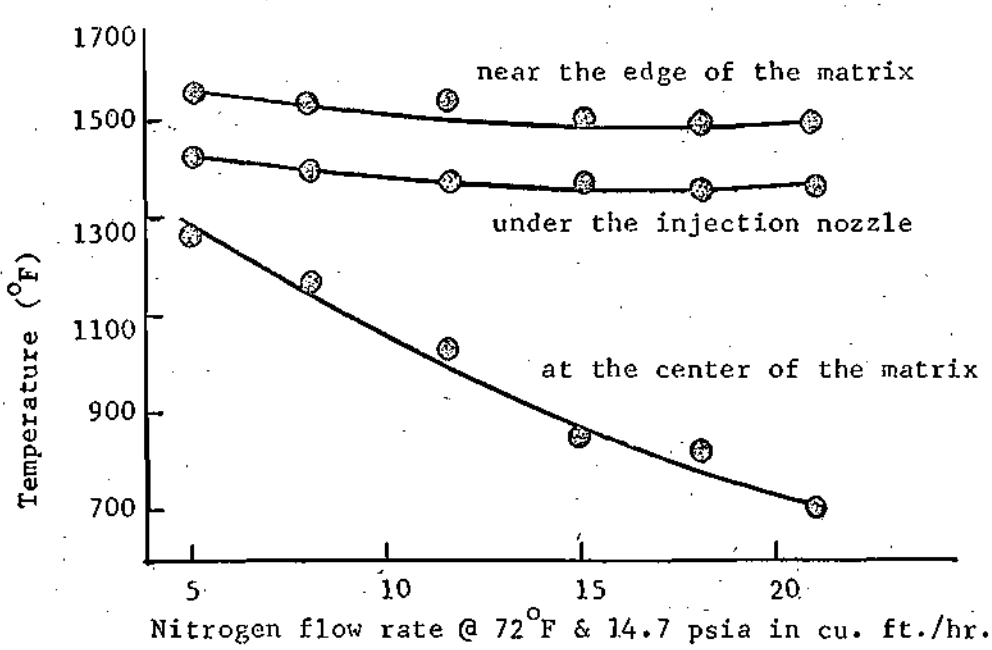

Figure A-2. Flat-Flame Temperature Variation with Opposed Nitrogen Flow; AF = 73.3.

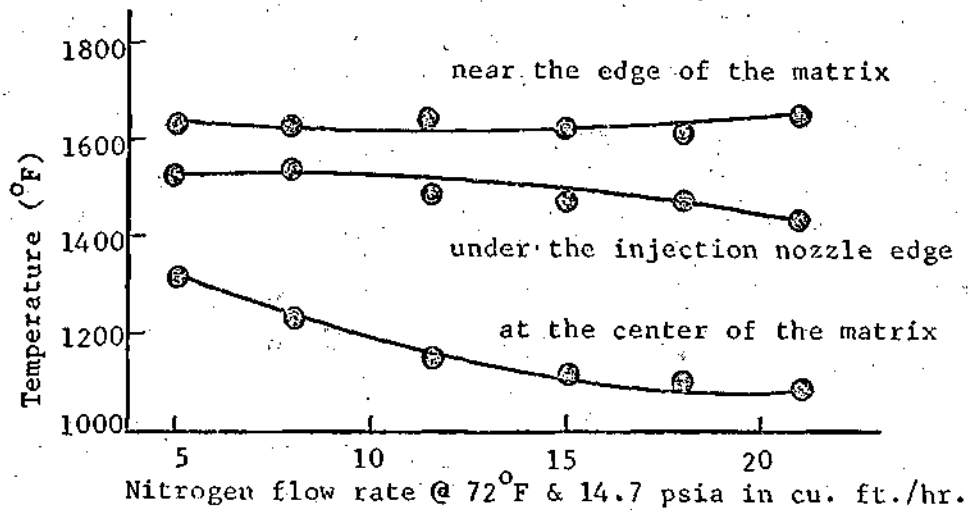

Figure A-3. Flat-Flame Temperature Variation with Opposed Nitrogen Flow; AF = 59.0.

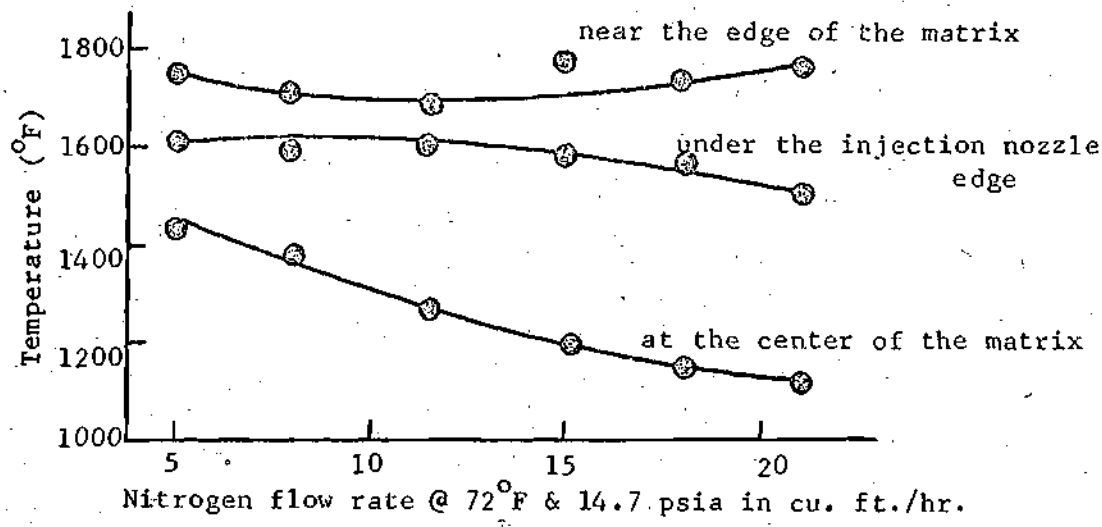

Figure A-4. Flat-Flame Temperature Variation with Opposed Nitrogen Flow; AF= 49.3.

Table A-2. Variation of Flat-Flame Temperature with Opposed Nitrogen Flow at Different Air-Fuel Ratios. (Figures 11, A-2, 12, A-1, A-3, A-4 & 13)

$\dot{V}_{N2}$ (ft ^{3}/hr) @ 72°F & 14.7 psia		5	8	11.5	15	18	21
AF $\frac{gm}{gm}$	r*	Flame Temperatures (°F)					
93.6							
	1	1529	1531	1531	1527	1530	
	2	1359	1355	1350	1352	1350	
	3	1064	820	553	475	431	
73.3							
	1	1563	1547	1552	1503	1503	1506
	2	1427	1400	1385	1372	1368	1362
	3	1270	1170	1032	863	822	700
68.25							
	1	1636	1636	1636	1636	1639	1637
	2	1530	1483	1470	1461	1450	1442
	3	1325	1182	1086	953	905	832
62.20							
	1	1694	1614	1616	1636	1652	1658
	2	1546	1537	1437	1392	1351	1340
	3	1296	1213	1101	1025	1006	1000
59.0							
	1	1634	1634	1652	1640	1630	1650
	2	1512	1540	1496	1476	1460	1435
	3	1306	1230	1152	1126	1105	1092
49.3							
	1	1763	1704	1699	1780	1740	1765
	2	1618	1596	1606	1585	1560	1520
	3	1433	1387	1278	1200	1159	1120
48.25							
	1	1787	1812	1806	1812	1800	1795
	2	1607	1587	1537	1530	1537	1524
	3	1376	1329	1343	1209	1168	1150

* r = Thermocouple position. Position 1 is about 0.3 inches from the edge of the flame; Position 2 is right under the nozzle edge, and Position 3 is at the center of the matrix.

Table A-3. Flame Temperature Variation with Opposed Nitrogen Flow on the Flame, AF = 52.2 and $\dot{m}_{N2} = 45.7 \times 10^{-3} \frac{gm}{sec}$. (Figure 14)

r* inches	Flame Temperature °F
0.0	1440
0.2	1796
0.4	1690
0.8	1480
1.2	1396
1.6	1277

* r = Radial distance from the matrix edge toward the center.

Table A-4. Flame Temperature Variation with Opposed Nitrogen Flow on the Flame, AF = 64, $\dot{m}_{N2} = 73.1 \times 10^{-3} \frac{gm}{sec}$. (Figure 15 and 22.a)

r* inches	Flame Temperature °F
0.0	1387
0.2	1709
0.4	1570
0.8	1477
1.2	1306
1.6	1230

* r = Radial distance from the matrix edge toward the center.

Table A-5. Hot Gas Temperature Measured at a Plane of 1.6 Inches Above the Flat-Flame, AF = 48.25 $\dot{m}_{N2} = 73.1 \times 10^{-3} \frac{gm}{sec}$. (Figure 16)

r* inches	Gas Temperature °F
-0.4	778
-0.2	1158
0	1591
0.2	1680
0.4	1681
0.6	1680
0.8	1636
1.0	1244

* The above data were obtained by the use of a single thermocouple in a plane parallel to the flat-flame. Edge of the matrix is chosen as a reference point and the thermocouple was rotated and positioned at the radial distances r as shown in Figure 16.

Table A-6. Flame and Hot Gas Temperature with Particle-Nitrogen Mixture Injection on the Flame, AF = 64, $\dot{m}_{N2}$ = 73.1 x 10^{-3} $\frac{gm}{sec}$, $\dot{m}_{Al}$ = 2.5 x 10^{-2} $\frac{gm}{sec}$ $\dot{m}_{N2}$ (through the powder feeder) = 36.5 x 10^{-3} $\frac{gm}{sec}$. (Figures 22.b and 23.b)

r (1) inches	Flame Temperature °F	Z (at r = 1 in) (2) inches	Hot Gas Temperature °F
0.0	1485	0.0	1956
0.2	1835	0.75	1858
0.4	1995	0.80	1779
0.8	1998	1.2	1662
1.2	1921	1.6	1420
1.6	1774		

(1) r = Radial distance from the matrix edge toward the center.

(2) Z = Vertical distance from the flame plane at constant r.

Table A-7. Hot Gas Temperature Measured Along the Injection Nozzle, AF = 52.2, $\dot{m}_{N2} = 73.1 \times 10^{-3} \frac{gm}{sec}$. (Figure 23.a)

Z* (at r = 1 inches) inches	Hot Gas Temperature °F
0.0	1600
0.2	1652
0.4	1642
0.6	1459
0.8	1396
1.0	1334
1.2	1265
1.4	1244
1.6	1201

* Z = Vertical distance from the flame plane at constant r (≅ 1.0 inch measured from the matrix edge).

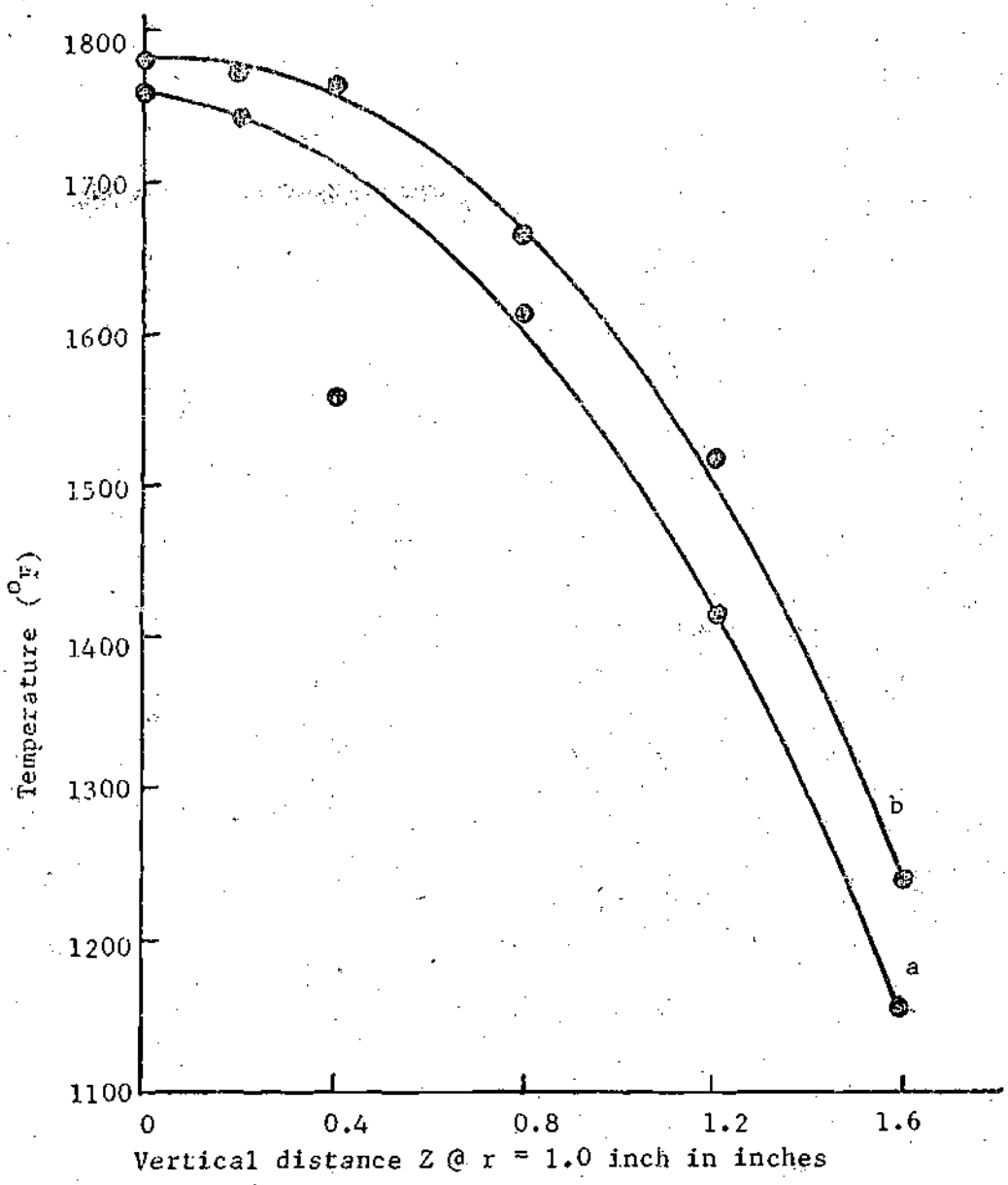

Figure A-5. Gas Temperatures with Nitrogen-Particle Flow in a Vertical Direction Measured Away from the Flame, AF = 52.2, $\dot{m}_{N2}$ = $45.7 \times 10^{-3} \frac{gm}{sec}$; (a) $\dot{m}_{Al} = 2.15 \times 10^{-2} \frac{gm}{sec}$; (b) $\dot{m}_{Al} = 2.25 \times 10^{-2} \frac{gm}{sec}$.

Table A-8. Hot Gas Temperatures with Particle-Nitrogen Mixture Injection on the Flat-Flame, AF = 52.2, $\dot{m}_{N2}$ = 45.7 x 10^{-3} $\frac{gm}{sec}$. (Figure A-5)

$\dot{m}_{N2}$ (1) $\frac{gm}{sec}$ x 10^3	$\dot{m}_{Al}$ $\frac{gm}{sec}$ x 10^2	Z (2) inches	Hot Gas Temperature °F
17.7	2.15		
		0.0	1760
		0.2	1743
		0.4	1560
		0.8	1613
		1.2	1415
		1.6	1158
25.3	2.25		
		0.0	1788
		0.2	1770
		0.4	1760
		0.8	1662
		1.2	1517
		1.6	1244

(1) $\dot{m}_{N2}$ = Nitrogen flow rate through the powder feeder.

(2) Z = Vertical distance from the flame plane at constant r (= 1.0 inches from the edge of the matrix).

APPENDIX B

SOME EMPIRICAL CORRELATION OF THE EXPERIMENTAL DATA

The data in the form of curves and profiles presented in this work shows a qualitative measure of the temperature in the reaction zone and its surrounding hot gases. As was mentioned in Chapter II the thermocouples have not been calibrated for radiation and heat losses; also the thermocouple bead looms large on the measured geometric scale of the flame zone thickness so that the measured temperature distribution misrepresents somewhat the actual temperature distribution through the combustion wave. Therefore, the utilization of these data for quantitative interpretation of the actual combustion processes is open to serious questions, although they are believed to be adequate for the qualitative interpretation. It being understood that conclusions arrived at in this way are tentative and will require further corroboration before they are finally accepted.

An equation of the form

$$\frac{Tu}{T_{a,o}} = \left[A \left(\frac{Vu}{V_{a,o}}\right) \left(\frac{1}{1+\lambda}\right)\right]^a \qquad (1)$$

(where A and a are constants, Vu is the observed flame velocity, $V_{a,o}$ is the air initial velocity, $T_{a,o}$ is the air initial temperature, Tu is the flame temperature, and λ is the air fuel ratio) which is basically arrived at by consideration of law of mass conservation,

can indeed correlate the data in the main portion of the undisturbed flat-flame. To see this, it is convenient to write equation (1) into a nondimensional logarithmic form as

$$\log T^* = B + \log V^* - a \log (1+\lambda) \tag{2}$$

where B is a constant equal to log A, $T^* = \frac{Tu}{T_{a,o}}$, and $V^* = \frac{Vu}{V_{a,o}}$. The observed flame velocity V_u is assumed to be equal to that of the outcoming gases and it is a constant. Therefore, equation (2) can be written in a final form as

$$\log T^* = C - a \log (1+\lambda) \tag{3}$$

where C is a constant. Equation (3) shows that the flame temperature is a function of only air-fuel ratio, and the flame planes are isothermal at each air-fuel ratio.

In order to fit the experimental data shown in Figure 8, it is necessary to evaluate the constants C and a of equation (3). However, values of C = 1.95 and a = 0.319 can best fit the data. A plot of the above equation is shown in Figure B-1.

Equation (3) shows the dependency of the flame temperature to the air-fuel ratio. It is a well established fact that the actual flame velocity is a function of only air-fuel ratio, then equation (3) can be considered as a special form of the following general equation.

$$\log T^* = \log [f (\lambda)] \tag{4}$$

In the case where the flames are disturbed by nitrogen, there are three regions of significance; a region of the flame where there

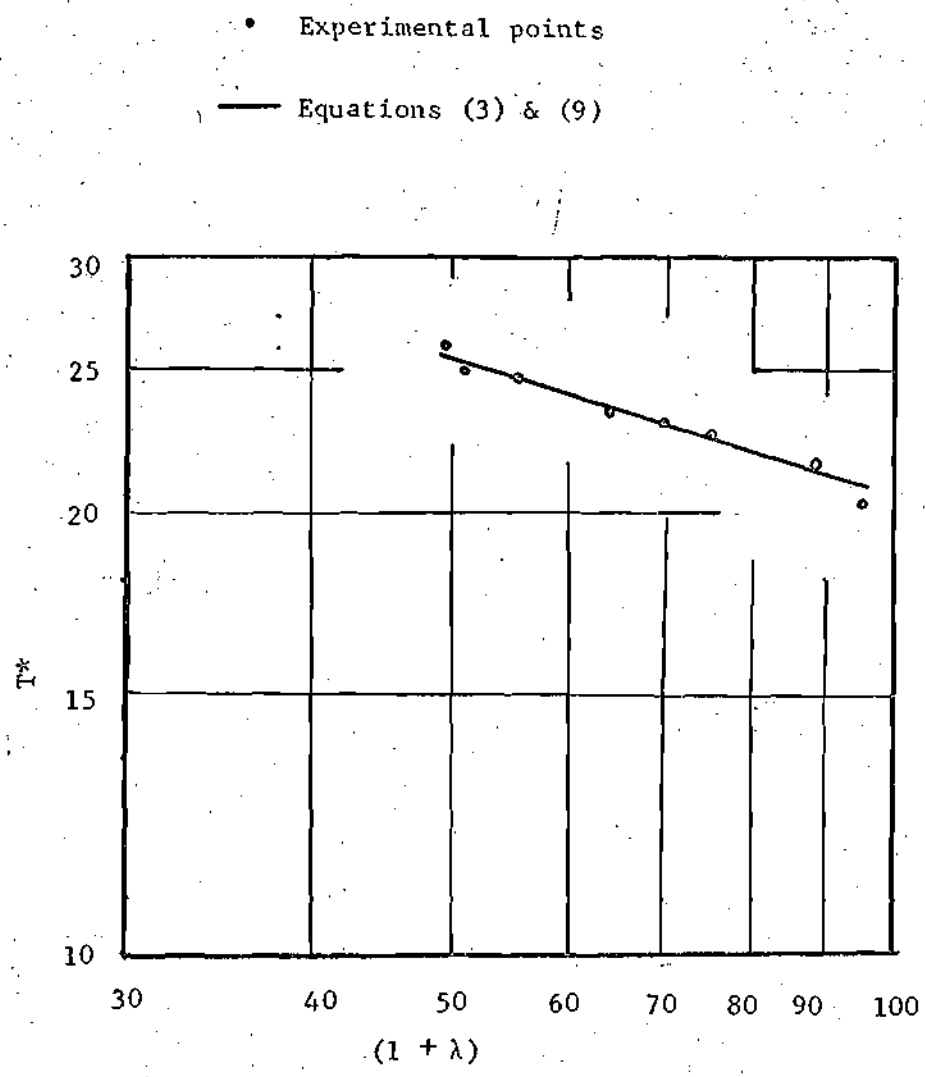

Figure B-1. Flame Temperature Variation as a Function of AF Ratio.

is no effect due nitrogen flow on the flame, a region where there is some effect due to nitrogen impingment on the flame and located between the periphery and the center of the flame, and the central portion of the flame where the interference is dominant. In all of the above cases, the temperature is a function of the air-fuel ratio and the mass flow rate of nitrogen.

$$T^* = F(\lambda, \frac{\dot{m}_{N2}}{\dot{m}_{a,o}}) \tag{5}$$

A function F to fit the temperature variation with nitrogen at the above three positions may have the form

$$T^* = F\ (\lambda,\beta) = [g(\lambda)][Ae^{-\beta}] \tag{6}$$

where

$$\beta = \frac{\dot{m}_{N2}}{\dot{m}_{a,o}} = \frac{\text{mass flow rate of } N_2 \text{ @ Tu \& 1 atm.}}{\text{mass flow rate of air @ } 70^oF \text{ \& } P_{a,o}} \tag{7}$$

and A is a constant.

Since the flow of nitrogen reverses in direction completely after impinging on the central portion of the flame, and it does not affect the regions close to the outer edge of the flame; the average flame temperature in this region is approximately the same as that of the undisturbed flat-flame, then β is zero in this region; equation (6) in the logarithmic form with the value of $\beta = 0$ become

$$\log T^* = \log [g(\lambda)] + \log A \tag{8}$$

Using the experimental data to evaluate equation (8), the result

became

$$\text{Log } T^* = 1.95 - 0.319 \text{ Log } (1 + \lambda) \tag{9}$$

which is identical to the one obtained from the plain undisturbed flat-flame and shown in Figure B-1.

This fact also shows that the outer portion of the flame remain virtually undisturbed by the impinging nitrogen within the flow rates used in this experimental work.

From the experimental curves, Figures 11, 12, 13, A-1, to A-4, the temperature variation at the central portion of the flame and its vicinity can be approximated by equation (6) which can be written in the following form

$$\text{Log } \left(\frac{1}{T^*}\right) = \beta + 0.319 \log (1+\lambda) - \beta^* \tag{10}$$

where β^* is a constant with a different value for each of the experimental curves.

Equations (3), (9), and (10) are the emperical equations resulting from a graphical fit to the data and are presented merely as a practicality and without any further comments.

APPENDIX C

FLOWMETER CALIBRATION CURVES

This appendix contains the calibration curves for air, nitrogen, and methane flowmeters. Powder feeder nitrogen flowmeter calibration and powder rate curves are also included.

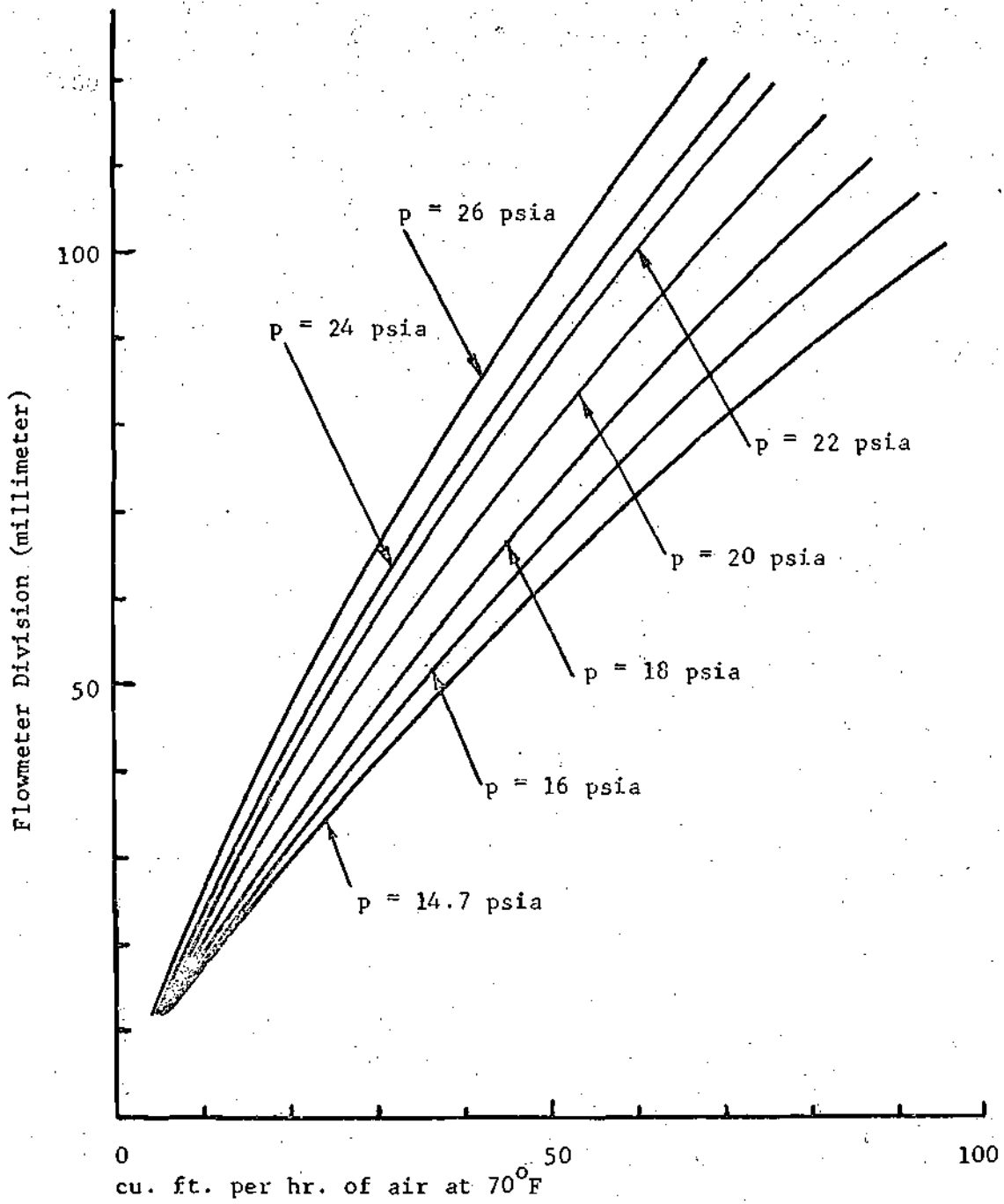

Figure C-1. Calibration Curve of Air Flowmeter.

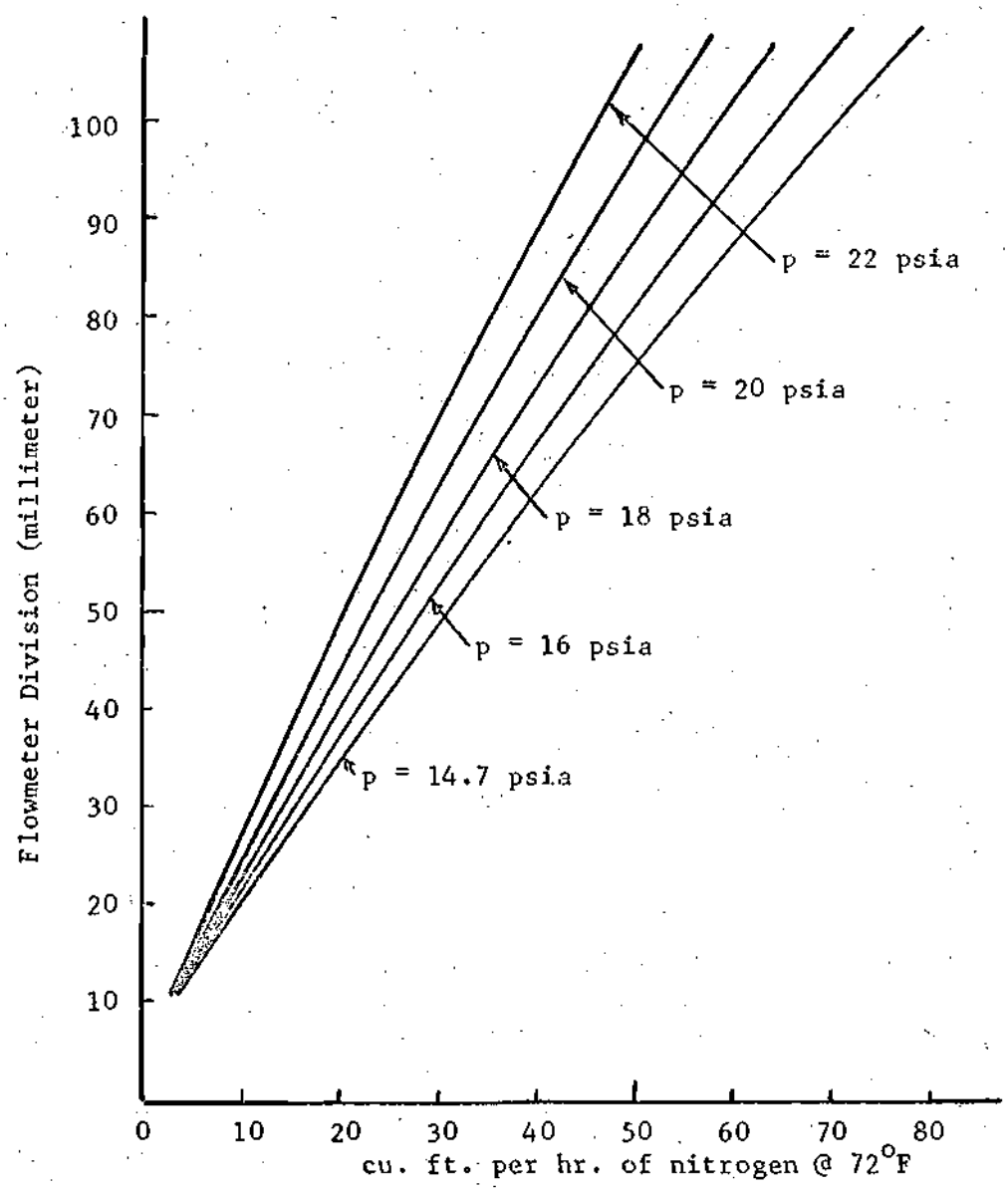

Figure C-2. Calibration Curve of Nitrogen Flowmeter.

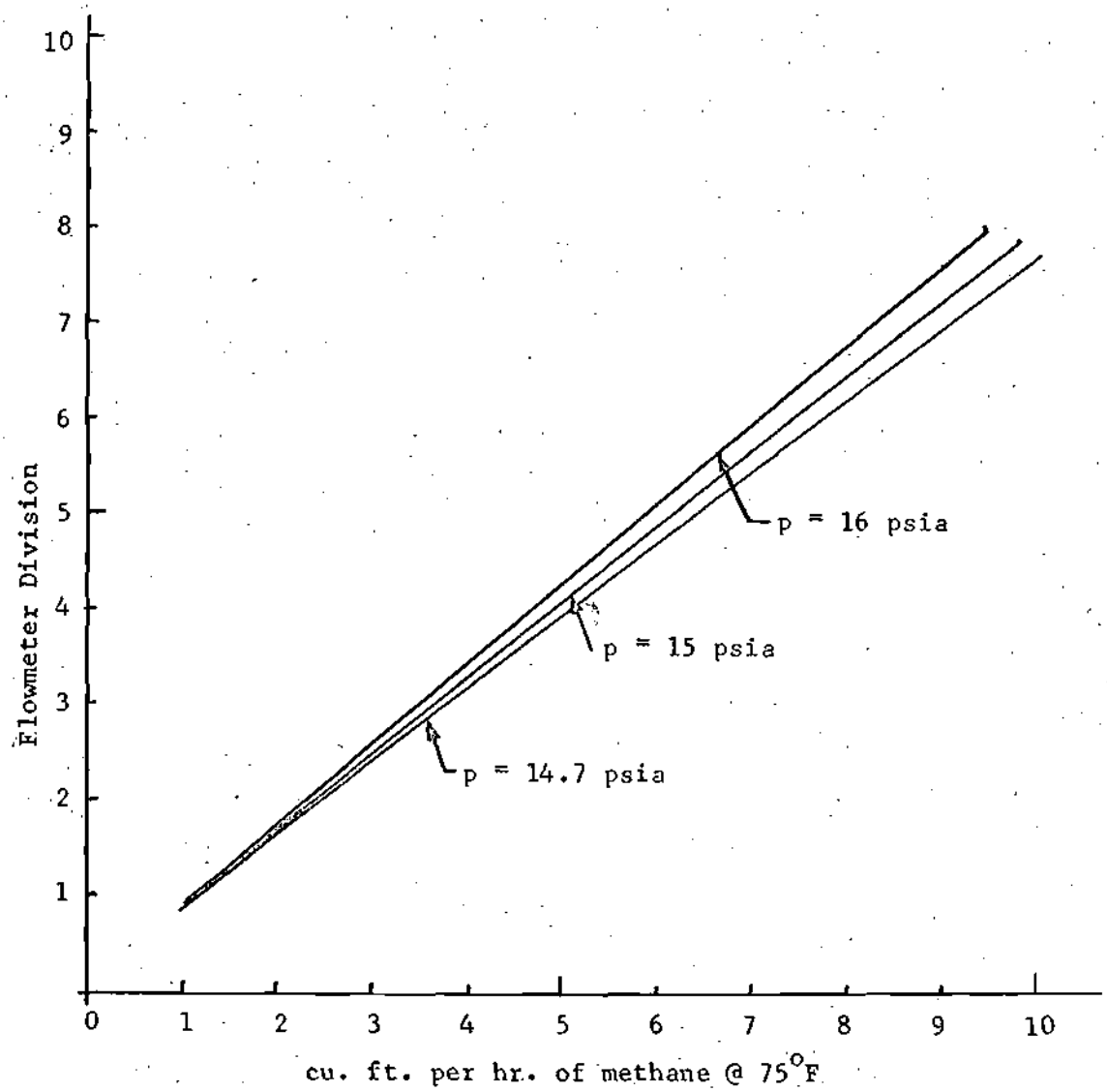

Figure C-3. Calibration Curve for Methane Flowmeter.

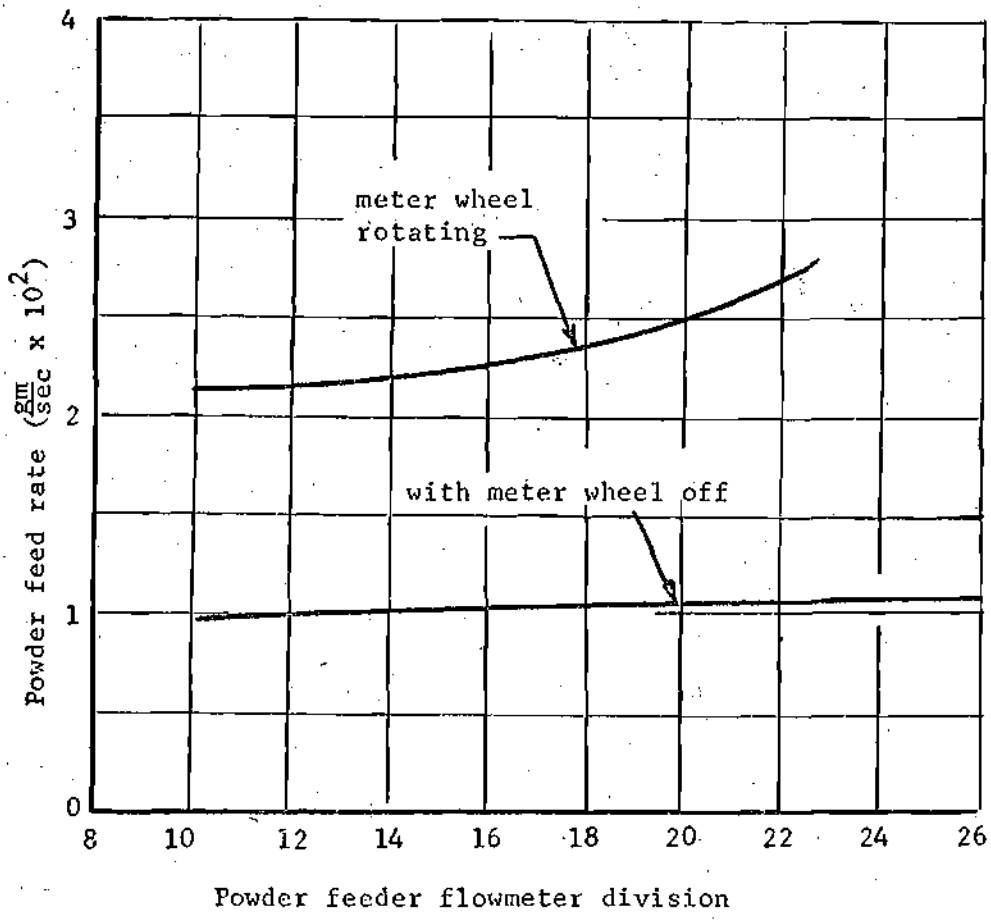

Figure C-4. Powder Feed Rate Drawn Against Nitrogen Flow Through the Powder Feeder.

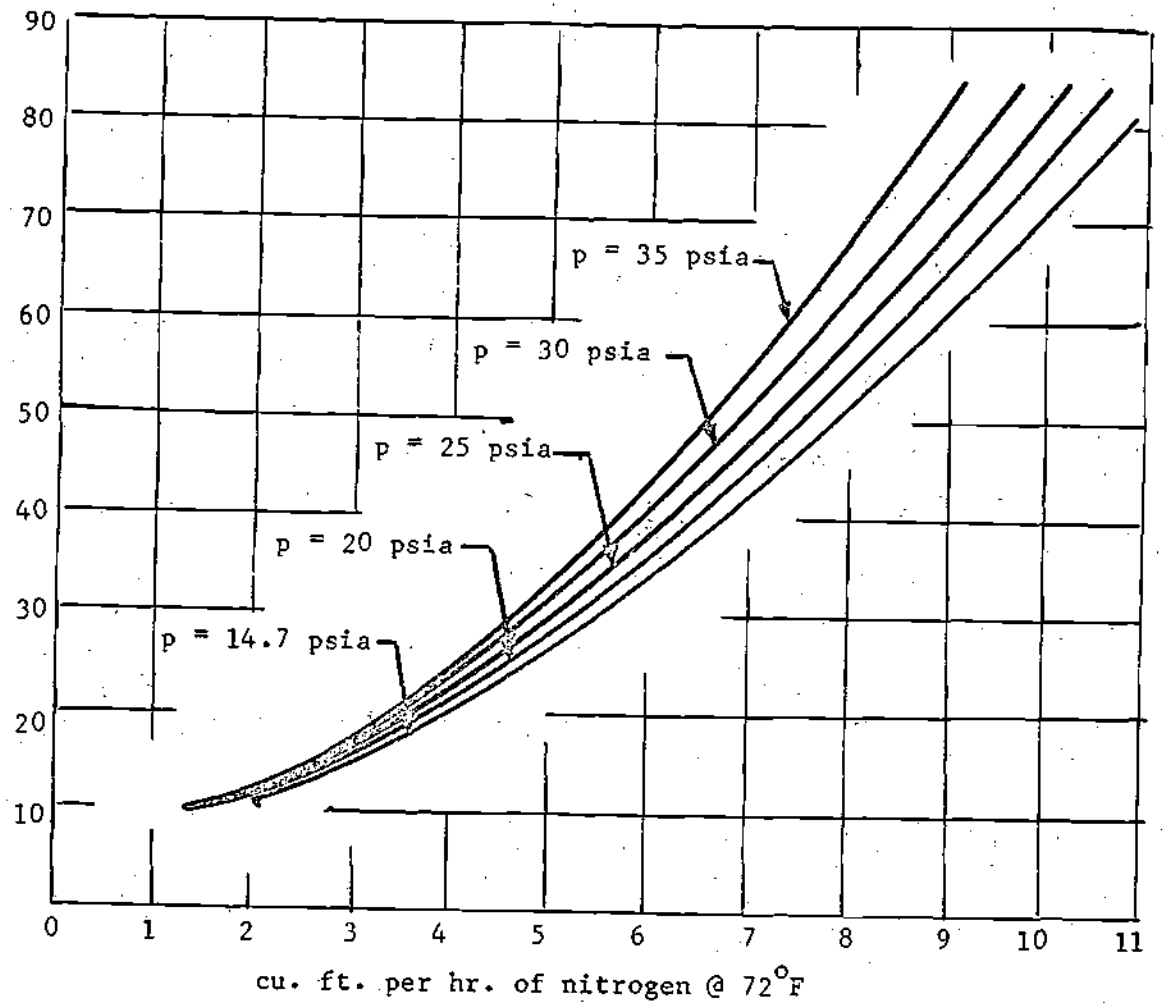

Figure C-5. Calibration Curve for the Flowmeter in the Powder Feeder for Nitrogen Flow.

BIBLIOGRAPHY

LITERATURE CITED

1. Da Rosa, A. V., "A Comparison of Relative Values of Fuel," ARS J. 14,4 (1945).

2. Markstein, G. H., "Combustion of Metals," AIAA J. 1, 550-562 (1963).

3. Christensen, H. C. Knipe, R. H., and Gordon, A. S., "Survey of Aluminum Particle Combustion," Pyrodynamics 3, 91-119 (1965).

4. Macek, A., "Fundamentals of Combustion of Single Aluminum and Beryllium Particles," Eleventh Symposium (International) on Combustion (Academic Press, New York, 1967) pp. 203-214.

5. Bahn, G. S., "On Pyrophoricity of Metals and of Fine Metal Powders in Particular," Pyrodynamics 3, 29-41 (1965).

6. Brandmaier, H. E., Particulate Cloud, (H. L. Green, and W. R. Lane Van Nostrand) pp. 383-386, Princeton, N. J., (1964).

7. Kuehl, D. K., "Ignition and Combustion of Aluminum and Beryllium," AIAA J. 3, 2239-2247 (1965).

8. Brzustowski, T. A., Glassman, I., "Spectroscopic Investigation of Metal Combustion," AIAA Progress in Aeronautics and Astronautics: Heterogeneous Combustion, Edited by Hans G. Wolfhard, Irwin Glassman, and Leon Green Jr. (Academic Press Inc., New York, 1964) Vol. 15, pp. 41-73.

9. Kuehl, D. K., "The Ignition and Combustion of Small Diameter Aluminum Wires," Pyrodynamics 3, 65-79 (1965).

10. Friedman, R. and Macek, A., "Ignition and Combustion of Aluminum Particles in Hot Ambient Gases," Combustion and Flame 6, 9-19 (1962).

11. Friedman, R. and Macek, A., "Combustion Studies of Single Aluminum Particles," Ninth Symposium (International) on Combustion, 703-709 (Academic Press Inc., New York, 1963).

12. Markstein G. H. "Heterogeneous Reaction in Metal Combustion," Eleventh Symposium (International) on Combustion (Academic Press, New York, 1967) pp. 219-233.

13. Brzustowski, T. A., "Vapor-Phase Diffusion Flames in the Combustion of Magnesium and Aluminum," Ph.D. Thesis, Princeton Univ., Dept. of Aeronautical Engineering (1963).

14. Brzustowski, T. A., and Glassman, I., "Vapor-Phase Diffusion Flames in the Combustion of Aluminum and Magnesium: I. Analytical Developments," Reference 38 pp. 75-115.

15. Brzustowski, T. A., and Glassman, I., "Vapor-Phase Diffusion Flames in the Combustion of Aluminum and Magnesium II," Reference 38, pp. 117-158.

16. Prentice, L. J., Drew, C. M., and Christensen, H. C., "Preliminary Studies of High Speed Photography of Aluminum Particles Combustion in Flames," Pyrodynamics 3, pp. 81-90 (1965).

17. Macek, A., Friedman, R., and Semple, J. M., "Techniques for Study of Combustion of Beryllium and Aluminum," Reference 38, pp. 3-16.

18. Drew, C. M., Gordon, A. S., and Knipe, R. H., "Study of Quenched Aluminum Particle Combustion," Reference 38, pp. 17-39.

19. Bartlett, R. W., Ong, J. N. Jr., Fassell, W. M. Jr. and Papp, C. A., "Estimating Aluminum Particle Combustion Kinetics," Combustion and Flame 7, pp. 227-234 (1963).

20. Bartlett, R. W., Combustion and Flame 8, pp. 341-342 (1964).

21. Gordon, D. A., "Combustion Characteristics of Metal Particles," ARS Progress in Astronautics and Rocketry: Solid Propellant Rocket Research, Edited by M. Summerfield (Academic Press, New York, 1960) Vol. I, pp. 253-257.

22. Davis, A., " Solid Propellants: The Combustion of Particles of Metal Ingredients," Combustion and Flame 7, pp. 359-367 (1963).

23. Fassell, W. M., Papp, C. A., Hildenbrand, D. L. and Sernka, R. P., ARS Progress in Astronautics and Rocketry: Solid Propellant Rocket Research, Edited by M. Summerfield (Academic Press, New York, 1960) Vol. I, pp. 259-270.

24. Drew, C. M., "Some Further Comments on the Paper, Estimating Aluminum Particle Combustion Kinetics," Combustion and Flame 9, pp. 205-208 (1965).

25. Brzustowski, T. A., Combustion and Flame 8, pp. 339-340 (1964).

26. Prentice, J. L., "On Combustion of Single Aluminum Particles," Combustion and Flame 9, pp. 208-210 (1965).

27. Kuehl, D. K., Eleventh Symposium (International) on Combustion (Academic Press Inc. New York, 1967) pp. 214-215.

28. Nelson, L. S., Prentice, J. L., and Richardson, N. L., "Apparatus for the Production and Ignition of Metal Droplets with a Pulsed Laser," Rev. Sci. Inst., 39, pp. 744-747 (1968).

29. Prentice, J. L., Eleventh Symposium (International) on Combustion (Academic Press Inc., New York, 1967) pp. 215-217.

30. Prentice, J. L., and Nelson, L. S., "Difference between the Combustion of Aluminum Droplet in Air and in an Oxygen-Argon Mixture," J. Electro Chem. Soc.: Electrochemical Science, Vol. 15, pp. 809-812, (1968).

31. Gordon, A. S., Eleventh Symposium (International) on Combustion (Academic Press, Inc., New York, 1967) p. 215.

32. AIAA Progress in Aeronautics and Astronautics: Heterogeneous Combustion, Edited by Hans G. Wolfhard, Irwin Glassman, and Leon Green Jr., Academic Press Inc., New York, (1964), Vol. 15, pp. 3-176.

33. ARS Progress in Astronautics and Rocketry: Solid Propellant Rocket Research, Edited by M. Summerfield, Vol. I, Academic Press, Inc., New York, (1960) pp. 253-291.

34. Pyrodynamics 3, Gordon & Breach Science Publishers Ltd. (1965) pp. 43-168.

35. Nelson, L. S., "Combustion of Zirconium Droplets by Flash Heating," Pyrodynamics 3, pp. 121-134 (1965).

36. Nelson, L. S., "Combustion of Metal Droplet Ignited by Flash Heating," Eleventh Symposium (International) on Combustion (Academic Press Inc., New York, 1967) pp. 409-415.

37. Nelson, L. S., "Nature of Spearpoints Observed in the Combustion of Zirconium Droplets," Nature 207, p. 741 (1965).

38. Nelson, L. S., "Possible Rate of Supercooling in the Spearpoints Observed during the Combustion of Zirconium Droplets," Nature 210 p. 410 (1966).

39. Nelson, L. S., Eleventh Symposium (International) on Combustion, p. 215 (1967).

40. Marshall, R. L., Nelson, L. S., and Richardson, N. L., "Luminus Fog Layer Surrounding a Zirconium Droplet Burning in an Oxygen Containing Atmosphere," Combustion and Flames 13, pp. 216-219 (1969).

41. Beal, J. L., Brown, W. R. and Vassalo, F. A., "Oxydation and Explosion of Drops of Molten Zirconium Metal," Pyrodynamics 3, pp. 135-160 (1965).

42. Rhein, R. A., "The Combustion of Powdered Metal in Nitrogen and Carbon-Dioxide," Pyrodynamics 3, pp. 161-168 (1965).

43. Morrison, M. E., and Scheller, K., "Spectral Characteristics of Hydrocarbon-Air Flames Containing Aluminum, Magnesium and Boron," Combustion and Flame 13, pp. 93-97 (1969).

44. Seleznev, V. A., Pokhil, P. F., Maltsev, V. M., and Bavykin, I. B., "An Optical Method of Measuring the Burning-Surface Temperature of Condensed Systems," Combustion and Flame 13, pp 139-142 (1969).

45. Marshall, R. L., Pellett, G. L., and Saunders, A. R., "An Experimental Study of the Drag Coefficient of Burning Aluminum Droplets," NASA TNX 59145-N 68-27406 (1966).

46. Powling, J., "The Flat Flame Burner," Experimental Method in Combustion Research, AGARD Manual, Section 2.2.1., pp. 14 Pergamon Press, New York (1961).

47. Levy, A., and Weinberg, F. J., "Conclusions Concerning Propagation of Flat Flames," Seventh Symposium (International) on Combustion, Butherwood Scientific Publications, London, pp. 296-305 (1959).

48. Heinsohn, R. J., "Studies of a Flat-Flame Under Impressed Electric and Magnetic Fields," Ph.D. Thesis, Michigan State Univ. Dept. of Mechanical Engin. 1963.

49. Heinsohn, R. J., and Lay, J. E., "Studies of a Flat-Flame Under Electric and Magnetic Fields," ASME 64-WA/ENER-2, (1964).

50. Egerton, A., and Thabet, S. K., "Flame Propagation: The Measurements of Burning Velocities of Slow Flames and the Determination of Limits of Combustion," Proc. Roy. Soc. A211 1952, pp. 445.

51. Friedman, R., "Measurement of the Temperature Profile in a Laminar Flame," Fourth Symposium (International) on Combustion, Baltimore: Williams and Wilkins, 1953, pp. 259.

52. Spalding, D. B., Botha, J. P., "Laminar Flame Speed of Propane-Air Mixtures with Heat Exchange from the Flame," Proc. Roy. Soc. A225, 1954, pp. 71.

53. Biedler, W. T., and Hoeslscher, H. E., "Studies in a New Type of Flat Flame Burner," Jet Propulsion, 27, 1957, pp. 1257.

54. Burgoyne, J., and Weinberg, F. J., "Determination of the Distribution of Some Parameters Across the Combustion Zone in a Flame Front," Proc. Roy. Soc. A224, 1954, p. 286.

55. Fristrom, R. M., and Westenberg, A. A., Flame Structure McGraw-Hill Book Company New York 1965 p. 104.

56. Egerton, A., and Sen, D., "Flame Propagation: The Influence of Pressure on the Burning Velocities of Flat Flames," Fourth Symposium (International) of Combustion, 1953.

57. Macek, A., Semple, J. M., "Experimental Burning Rates and Combustion Mechanism of Single Beryllium Particles," Twelfth Symposium (International) on Combustion, the Combustion Institute, 1969, pp. 71-79.

58. Bowen, M. D., "Personal Communication."

ADDITIONAL REFERENCES

Berkowitz-Mattuck, J. B., Bachler, A., Engelke, J. L., and Goldstein, S. N., J. Chem. Phys. 39, 2722 (1963).

Borgianni, C., Capitelli, M., Cramarossa, F., Triolo, L., and Molinari, E., "The Behavior of Metal Oxides Injected into an Argon Induction Plasma," Combustion and Flame 13, pp. 181-194 (1969).

Coffin, K. P., and Brokaw, R. S., "A General Lystem for Calculating Burning Rates of Particles and Drops and Comparison of Calculated Rates for Carbon, Boron, Magnesium, and Isooctane," NACA TN 3929 (1957).

Glassman, I., "Combustion of Metals-Physical Consideration," pp. 253-257, Reference 39.

Gulbransen, E. A., Andrew, K. F., and Brassart, F. A., pp. 227-250, Reference 38.

Mellor, M., and Glassman, I., "A Physical Criterion for Metal Ignition," pp. 43-64, Reference 40.

Michel, D., Perez, Y. Yorba, M., and Collongues, R., Compt. Rend. C263, p. 1366 (1966).

Nelson, L. S.: Science 148, p. 1594 (1965).

Reynolds, W. C., "Investigation of Ignition Temperature of Solid Metals," NASA TN-D-182 (1959).

Singer, J. M., and Liebman, I., "Spherical Flames of Spark Ignited Dust Clouds," Combustion and Flame 12, 506-509 (1968).